Carey

KRAKATAU VOLCANO EXPEDITION 1990
REPORT TO THE NATIONAL GEOGRAPHIC SOCIETY

Haraldur Sigurdsson, Steven Carey, Charles Mandeville
Graduate School of Oceanography, University of Rhode Island, Narragansett, R.I. 02882, USA

and

Sutikno Bronto
Volcanological Survey of Indonesia, Bandung, Indonesia

August 1990

Table of Contents

Cover: The new island of Calmeyer which formed in the Sunda Straits northeast of Krakatau as a result of the 1883 explosive eruption. The circular crater in the middle has been interpreted as forming from explosions caused by the interaction of hot, pyroclastic flows and seawater. The island is now underwater and was one of the areas explored by SCUBA diving during the 1990 expedition. From the chromolithograph plate 19 in Verbeek (1885).

Introduction

The 1883 eruption of Krakatau in the Sunda Straits of Indonesia is one of the largest explosive volcanic events in historic time and is surpassed only by the great 1815 Tambora eruption on the eastern Indonesian island of Sumbawa. Tsunamis or tidal waves generated by the Krakatau eruption were in excess of 35

m high on the coasts of Java and Sumatra and led to the loss of more than 36,000 lives. The eruption is of particular importance because of the large loss of life, far-reaching climatic perturbations and other atmospheric effects. Climatic records indicate that the Krakatau eruption caused global environmental effects by the injection of enormous quantities of volcanic aerosols into the Earth's stratosphere. The global-scale effects are manifested in such diverse records as acidity peaks in Greenland and Antarctic ice cores (Hammer et al., 1980; Clausen and Hammer, 1988), temperature records, and reduced growth and frost damage in long-lived species of North American and European trees (LaMarche and Hirschboeck, 1984; Papp, 1983). A study of the eruption is thus critical to an understanding of the response of the Earth's climate system to volcano-induced changes in the atmospheric heat budget.

The 1883 eruption of Krakatau is perhaps the best known of all explosive volcanic eruptions, yet paradoxically it is one of the most poorly understood. Fundamental questions remain unanswered regarding the height of the eruption plume, the total erupted mass, mass eruption rate and the role of submarine pyroclastic flows and/or debris flows in generating the catastrophic and lethal tsunamis. New research which incorporates current volcanological theories with field studies of the pyroclastic deposits has demonstrated that a key element was the interaction of subaerially-generated pyroclastic flows with the surrounding sea (Self and Rampino, 1981).

In 1990 we carried out a detailed study of the deposits from this important eruption, in order to provide answers to these fundamental questions. The study was conducted in collaboration with Dr. Sutikno Bronto of the Volcanological Survey of Indonesia, and included both land-based studies of volcanic deposits on islands in the Sunda Straits and marine-based studies of the seafloor adjacent to the Krakatau island group. The marine-based studies utilized SCUBA diving to collect submarine pyroclastic deposits from the 1883 eruption and bathymetric surveying to map out the undersea topography of the Krakatau caldera. Funding for the research was provided by grants from the National Geographic Society and the U.S. National Science Foundation. This report presents a preliminary summary and synthesis of the findings of our expedition. It is anticipated that the results of the study will form a valuable contribution towards an understanding of

hazardous volcanogenic tsunamis and aid in evaluation of atmospheric effects and other global environmental impacts of large explosive eruptions.

The 1883 Eruption

Prior to the 1883 eruption, the Krakatau volcanic complex of the Sunda Straights consisted of three main islands: Krakatau in the south, Sertung to the west, and Panjang in the east (fig. 1). The largest of the islands, Krakatau, was formed from three overlapping volcanic cones, Perboewatan, Danan and Rakata, aligned along a northwest to southeast trend and each increasing successively in altitude up to 832 m at the southern peak of Rakata. Eruptive activity in 1883 began with an explosive eruption from the Perboewatan vent on 20 May. Several loud explosions associated with this event were heard up to 150 km away and a column of steam and ash was reported to have reached an altitude of 11 km. Ships that were in the area of Krakatau encountered rafts of floating pumice at a distance of 30 miles from the volcano on 22 May.

During the next three months minor explosive eruptions continued intermittently with light ashfall occurring on Krakatau and its neighboring islands. In July activity was taking place at vents near both Perboewatan and Danan. On 11 August, a Dutch surveyor, H.J. Ferzenaar, was the last person to visit Krakatau before the paroxysmal eruption. He noted that there were three active craters at that time and that only about 50 cm of ash had accumulated near the Perboewatan and Danang vents as a result of the three months of low level eruptions. On the morning of 26 August the intensity of explosive eruptions began to increase and a large convective ash column was generated over the island by a series of numerous explosions. The eruption changed character dramatically on the 27 August, when the first of five enormous explosions took place. These explosions were precisely recorded by pressure gauges at the gasworks in Jarkata. Self and Rampino (1981) have proposed that each of the explosions was associated with the generation of a pyroclastic flow that was discharged into the sea.

Following the eruption on 27 August, dramatic changes of the island group became evident (fig. 1). The majority of Krakatau island had disappeared and there was now a deep (270 meter) caldera in its place. Equally spectacular changes occurred on the sea floor in the Sebesi Channel, north and northeast of the

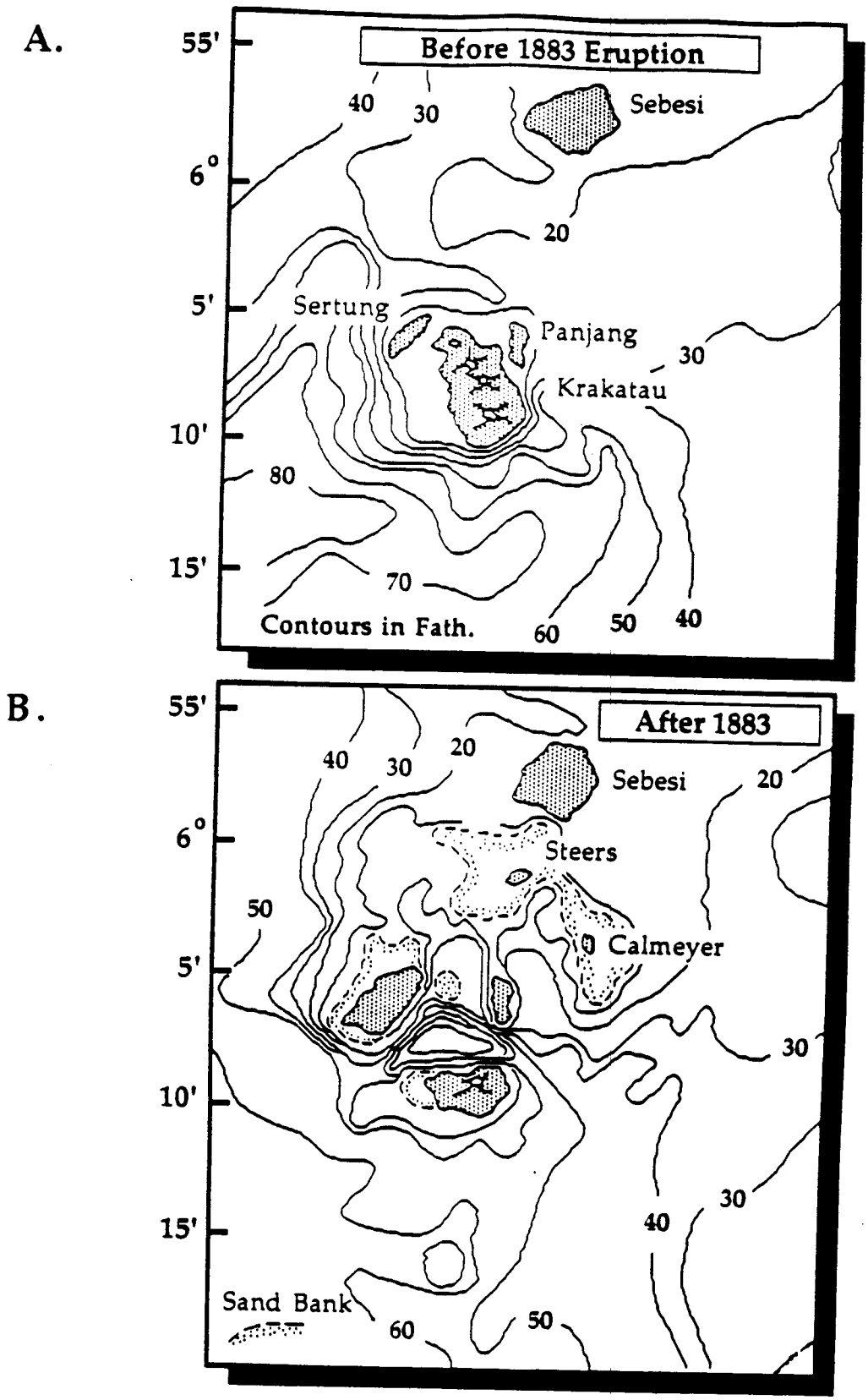

Fig. 1. Topographic and bathymetric changes resulting from the 1883 eruption of Krakatau volcano, Indonesia. Contours in fathoms. Stippled regions are sand banks at or near sea level, which emerged during the 1883 eruption as a result of pyroclastic flows advancing into the sea.

volcano. Two new ephemeral islands, Steers and Calmeyer, were formed within a 220 km^2 area to the north of the volcano which had decreased in depth by about 30 m (fig. 1). They protruded to only 3 and 6.5 meters above sealevel respectively, but by September both had been eroded to just below high tide level. Self and Rampino (1981) have proposed that this shoaling was due to the emplacement of pyroclastic flows generated during the climax of the eruption.

The eruption column height attained during the Krakatau eruption is unknown, but the volcanic cloud spread rapidly around the globe in the equatorial region, and the northward movement of the stratospheric cloud was about 70 km/day (Wexler, 1951). While the total erupted mass has been estimated as $2.7x10^{13}$ kg of dacitic magma, the volcanic degassing to the atmosphere has been estimated as $2.9x10^6$ tons H_2SO_4 and $3.8x10^6$ tons HCl on basis of analysis of glass inclusions in phenocrysts from the tephra (Devine et al. 1984). Climatological records indicate a northern hemisphere surface temperature decrease of 0.3 ^oC in the wake of the eruption (Rampino and Self, 1982; Jones et al. 1981). This is supported by tree ring evidence from North America and Europe, which indicates notable frost events and stunted growth, particularly in 1884 (LaMarche and Hirschboeck, 1984; Papp, 1983). The estimates of stratospheric sulfur aerosol mass and climate response for Krakatau are in agreement with the general correlation between these parameters in a data set of climate-modifying volcanic eruptions (Sigurdsson, 1989). However, a much better estimate of total erupted mass is required for the Krakatau event in order to substantiate this correlation.

One of the most important aspects of the eruption was the generation of tsunamis which claimed the lives of 36,000 people along the coasts of Java and Sumatra. The origin of these tsunamis remains controversial and is intimately linked to a general model for the eruptive processes during the cataclysmic phase. Three hypotheses have been put forward to explain the tsunamis:

1. Large-scale collapse of the northern part of Krakatau island and generation of debris flows into the sea (Verbeek, 1885; Self and Rampino, 1981; Camus and Vincent, 1983)

2. Submarine explosions related to the interaction of magma and seawater (Yokoyama, 1981,1987)

3. Discharge of subaerially-generated pyroclastic flows into the sea (Latter, 1981; Self and Rampino, 1981; Verbeek, 1885)

One of the major objectives of our marine-based studies at Krakatau was to make observations and obtain samples that could be used to test these various hypotheses. There were no existing samples of the seafloor adjacent to the Krakatau island group in the Sunda Straits prior to our study. This is remarkable in view of the great importance of the 1883 eruption to volcanology and climatology. Our marine studies were guided by the following assumptions: if (1) is the correct hypothesis, then the shallow area to the north of the volcano should consist of the collapsed parts of the old volcanic edifice. On the other hand, if model (3) is correct then the shallow area should consist largely of pyroclastic flows rich in juvenile magmatic components. Preliminary support for model (3) comes from lithographs of Steers and Calmeyer islands (Verbeek, 1885) which suggest that they consist of light-colored pyroclastic flows and show evidence of pseudocraters. In addition, similar lithographs of Sebesi island, northeast of Krakatau, indicates that virtually all of the vegetation was stripped off by a powerful pyroclastic flow that deposited about 1.5 m of light colored ash and pumice.

Logistics of the Expedition

The Krakatau volcanological expedition was carried out from 9 April to 11 June, 1990. Members of the expedition were: Dr. Haraldur Sigurdsson, Professor of Oceanography, Dr. Steven Carey, Assistant Professor of Oceanography, Mr. Charles Mandeville, Graduates Student, all from the University of Rhode Island; Ms. Jean M. Sigurdsson, assistant, and Dr. Sutikno Bronto, Volcanological Survey of Indonesia, Bandung.

The present Krakatau island group is made up of four islands: Sertung in the west, Rakata in the south-east, Panjang in the east and Anak Krakatau in the center, formed as a result of post-1883 volcanic activity at north rim of the submarine caldera. These islands have been designated a National Park by the Government of Indonesia, and this nature preserve is uninhabited, except for four forestry officials who reside on the island of Sertung. In order to carry out geological research in this area, clearance was obtained through LIPI, the Indonesian Scientific Research Department, and the Department of Natural

Resources. Because of the remote location of the Krakatau island group in the Sunda Straits, about 40 km west of Java, we established a primary base camp on the island of Sertung, from which we carried out both the land and marine-based components of the expedition.

During the expedition we chartered at various times the motor vessels M/V Muitara, Rapala and Simpati for inter-island transport, SCUBA diving support and bathymetric surveying. M/V Simpati was in our service during most of the expedition, whereas the other two vessels were chartered during diving periods only. We are very grateful to Mr. Gatot Sudarto of Kalpataru, Mr. Agoestono of Labuan and the crews of their boats for the excellent services rendered at sea and on land.

Land-based Studies

During the expedition, we examined the volcanic stratigraphy of the Krakatau island group, and studied far-travelled deposits from the 1883 eruption on other islands in the Sunda Straits, as well as along the Sumatra coast to the north. Our objectives were to 1) identify and map out the distribution of different pyroclastic deposit facies, i.e. fall, flow or surge, 2) establish the temporal evolution of volcanic processes as recorded in the stratigraphic succcession of pyroclastic deposits, 3) collect data on the dispersal of clasts to be used to infer aspects of eruption dynamics, and 4) assess the nature of pre-1883 explosive activity of the Krakatau islands.

A. Proximal Deposits from the 1883 Eruption

The base of the 1883 volcanic deposits is exposed at a number of locations on the islands of Panjang, Sertung and Rakata. We studied the basal contact and overlying 1883 deposits at two sites on east Rakata, at one site on west Rakata, at two sites on east Sertung, and at five sites on south, east and west Panjang island. The following table and figure 2 summarizes the general proximal stratigraphic succession of the 1883 deposits on the Krakatau islands:

Proximal Stratigraphy of 1883 Krakatau Deposits:

---

9. Grey to dark grey pyroclastic flow unit, extremely lithic-rich, with abundant dense lithic lava blocks up to 2 m in diameter. Probable lag deposit from a major pyroclastic flow.
8. Grey to light grey pyroclastic flow succession, consisting of at least four major flow units. Individual flows range in thickness from 4 to 20 m.
7. Light grey, lithic-rich plinian pumice fall deposit, from 10 to 38 cm thick.
6. Grey to dark grey pumice-rich pyroclastic surge deposit, ranging from massive to crudely stratified and cross-bedded in some exposures; thickness up to 70 cm.
5. Grey, lithic-rich plinian pumice fall deposit, ranging in thickness up to 91 cm on the Krakatau islands; the layer is coarser than the earlier plinian fall (layer 3 below), with up to 30 cm diameter pinkish grey pumice clasts and 17 cm lithics.
4. Grey, poorly sorted, pumice lapilli deposit, ranging in thickness form 10 to 50 cm. Contains charcoal; internal structures include crude stratification and minor cross-bedding at some localities. The layer is probably a pyroclastic surge, but at south end of Panjang island this layer grades laterally into 90 cm thick pyroclastic flow channel fill.
3. Light grey, lithic-rich plinian pumice fall, moderately to well sorted, typically 5 to 20 cm thick on the Krakatau islands. Contains pinkish grey pumice clasts up to 20 cm and 5 cm diameter lithic clasts.
2. Grey silty-sandy ash, massive and well sorted, 3 to 20 cm thick, which contains scattered light grey pumice clasts.
1. Olive grey, massive silty ash fall, moderately to well sorted and contains up to 5 mm diameter accretionary lapilli and common plant impressions. Ranges in thickness from 2 up to maximum of 22 cm on south-western part of Rakata. Matrix of this fall is slightly vesicular in some exposures.

Pre-1883 brown silty soil at base.

Proximal 1883 Krakatau Stratigraphy

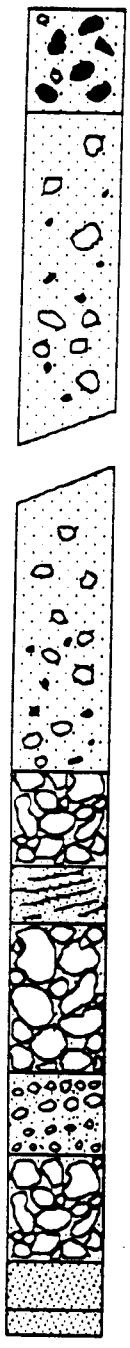

Unit Number

9 Grey to dark grey pyroclastic flow unit with dense lithic blocks up to 2 m in diameter

8 Grey to light grey pyroclastic flow succession with at least four major flow units

7 Light grey, lithic-rich plinian pumice fall

6 Grey, pumice-rich pyroclastic surge deposit

5 Grey, lithic-rich pumice plinian pumice fall

4 Grey pumice lapilli with crude stratification

3 Light-grey plinian pumice fall

2 Grey silty-sandy ash fall

1 Olive grey, silty ash fall

Fig. 2. Composite stratigraphic relations of the 1883 pyroclastic deposits of Krakatau volcano based on examination of proximal localities. See text for complete descriptions of each unit.

The proximal stratigraphy can be used to infer the evolution of volcanic processes during the great 1883 eruption and to correlate specific pyroclastic units to historical accounts of the event. Just above the 1883 soil are two, relatively thin ash fall deposits that we attribute to the initiation of volcanic activity at Krakatau in May of 1883 and the continued low level explosive eruptions which occurred sporadically during the months of June, July and the first part of August. The fine grained nature of these layers and the occurrence of accretionary lapilli suggest that some of the activity was phreatomagmatic, i.e. resulting from the interaction of magma with external water.

The onset of the paroxsymal eruption on 26 August can be correlated to the pumice fall unit 3 (fig. 2). This deposit indicates that a large convective eruption column in excess of 20 km high had developed over Krakatau and that a rain of pumice and ash was blanketing the surrounding islands. Sightings from the ship *Medea* , located 76 miles east northeast of Krakatau on the afternoon of 26 August, indicate an eruption column extending up to 26 km at 2:00 pm local time (Simkin and Fiske, 1983). During this time small volume pyroclastic surges and flows were generated and spread at least to the east and southeast (unit 4). We suspect that these pyroclastic density currents were produced from local instabilities in the eruption column margin and do not represent a complete shift from a dominantly convecting column to a collapsing one. Following the generation of these flows there was once again a return to heavy pumice and ash fallout from a sustained eruption column (unit 5). This period was again interrupted by the generation of pyroclastic surges (unit 6) but reverted to pumice fall prior to the transition to major pyroclastic flows (unit 8).

Historical accounts indicate that a major shift in eruptive acitivity occurred on 27 August when a series of enormous explosions were recorded. The largest took place at about 10:00 am and was associated with a destructive tsunami that inundated the west coast of Java and resulted in the loss of thousands of lives. Ships that were located northeast of Krakatau reported seeing a large dark front rise up in the vicinity of the volcano and move swiftly towards them. The barque *W. H. Besse* experienced hurricane force winds 75 km from the volcano, that carried sand size volcanic ash (Simkin and Fiske, 1983). However, as the cloud struck the ship the water remained smooth and the smell of sulphur was very

strong. This description suggests that the "squall" was in fact the distal part of a dilute pyroclastic density flow that originated at Krakatau and spread out to the north and northeast. Other reports from this time period note the fallout of mud rain in addition to the dry fallout of volcanic ash. We interpret this period of severe explosions, tsunami generation, dry ash fallout and mud rain to the generation of large volume pyroclastic flows that entered the sea around Krakatau. This activity is marked by the transition from unit 7 (pumice fall) to unit 8 (pyroclastic flow series, fig. 2).

Self and Rampino (1981) have also studied the proximal stratigraphy of the 1883 deposits of the Krakatau eruption . Our results are in general agreement with their findings although there are some important differences. For example, both studies indicate that prior to the onset of major pyroclastic flow generation there was a period during which a large convective eruption column was developed over Krakatau and the fallout of ash and pumice produced coarse pumice fall deposits. However, Self and Rampino report that two of the early, thick pumice fall deposits were incipiently welded. During our studies, we found no evidence for welded fall deposits in the 1883 sequence. Welded pyroclastic deposits were observed on the south and southeast coast of Panjang but stratigraphic relations clearly indicate that these deposits were associated with eruptions prior to 1883. It may be that Self and Rampino have confused these earlier deposits with the 1883 stratigraphic sequence.

B. Distal Deposits from the 1883 Eruption

Contemporary reports of the 1883 eruption indicate clearly that the event had severe impact on the islands of Sebesi and Sebuku north of the volcano and on the south coast of Sumatra. Reports of the thickness of ash on these islands range from 0.6 to 1.5 m (Verbeek, 1885), and up to 30 cm on the south coast of Sumatra. Historical reports also indicate that these distal ash deposits were formed by some type of hot density current, and not from fallout, as shown by the loss of over 2,000 lives by burns on the Sumatra coast (Simkin and Fiske, 1983). Direct observations of these high-temperature ash clouds were made by the surviving Beyerinck family (Verbeek, 1885), and the evidence strongly indicates that these phenomena are due to the emplacement of hot pyroclastic flows and surges across the Sunda

Straits. Prior to our expedition there had not been any geological studies of the deposits in this area. We studied the pyroclastic deposits from the 1883 eruption on Sebesi, Huismans Island, Sebuku Kecil (Beschutters Island), Sebuku, Lagoendi, and on the south coast of Sumatra, around Rajabassa volcano (fig. 3), and the following are our observations on each island. Documentation of these deposits and their effects is of great importance in evaluating the potential volcanic hazards from future eruptions of the Krakatau island group.

The island of Sebesi is about 20 km NNE of Krakatau volcano (fig. 1), and the 1883 eruption led to complete devastation of this island, with all vegetation destroyed and trees reduced to stumps up to the 859 m high peak of this extinct volcano and buried in thick ash (Simkin and Fiske, 1983, p. 141). Over 3,000 lives were lost on this island. When Verbeek (1885) visited Sebesi island two months after the eruption, the pyroclastic deposit was 1 to 1.5 m thick, with rare "pieces the size of a head", and only tree stumps protruded from the ash.

We studied the 1883 pyroclastic deposit in six exposures on north and east Sebesi (Leganada, Tejang and Segenom), and found it to range in thickness from 83 to 260 cm. We found no evidence of a pumice or ash fallout layer on Sebesi or the other islands north of Krakatau. In southern part of the island, the 1883 deposit is generally composed of three units of poorly sorted, grey pumice-rich ash, ranging from massive to crudely stratified. Pumice clasts are generally 1 to 7 cm in diameter, and lithics of the order 0.5 to 1 cm. These units have the characteristics of pyroclastic surges or distal pyroclastic flows. Further north the lowermost unit is overlain by one or two units of well-sorted pumice lapilli, containing well rounded clasts of light grey pumice up to 4 cm in diameter, and virtually matrix- and lithics-free, ranging in thickness from 5 to 24 cm. These units probably represent pyroclastic surge or flow deposit, which may have been eroded and re-deposited by the tsunamis which accompanied the eruption. The reworked pumice units are overalin by two thick pyroclastic surge units in north Sebesi. These results indicate that the main tsunami(s) at about 10 am on 27 August, 1883, were preceded by at least one major pyroclastic flow event, and that they were accompanied by or followed by at least two pyroclastic flowage events.

On Sebuku and Sebuku Kecil (30 km NNE of Krakatau, fig. 3) the islands were reported to be "almost completely buried under ash. Only on the highest

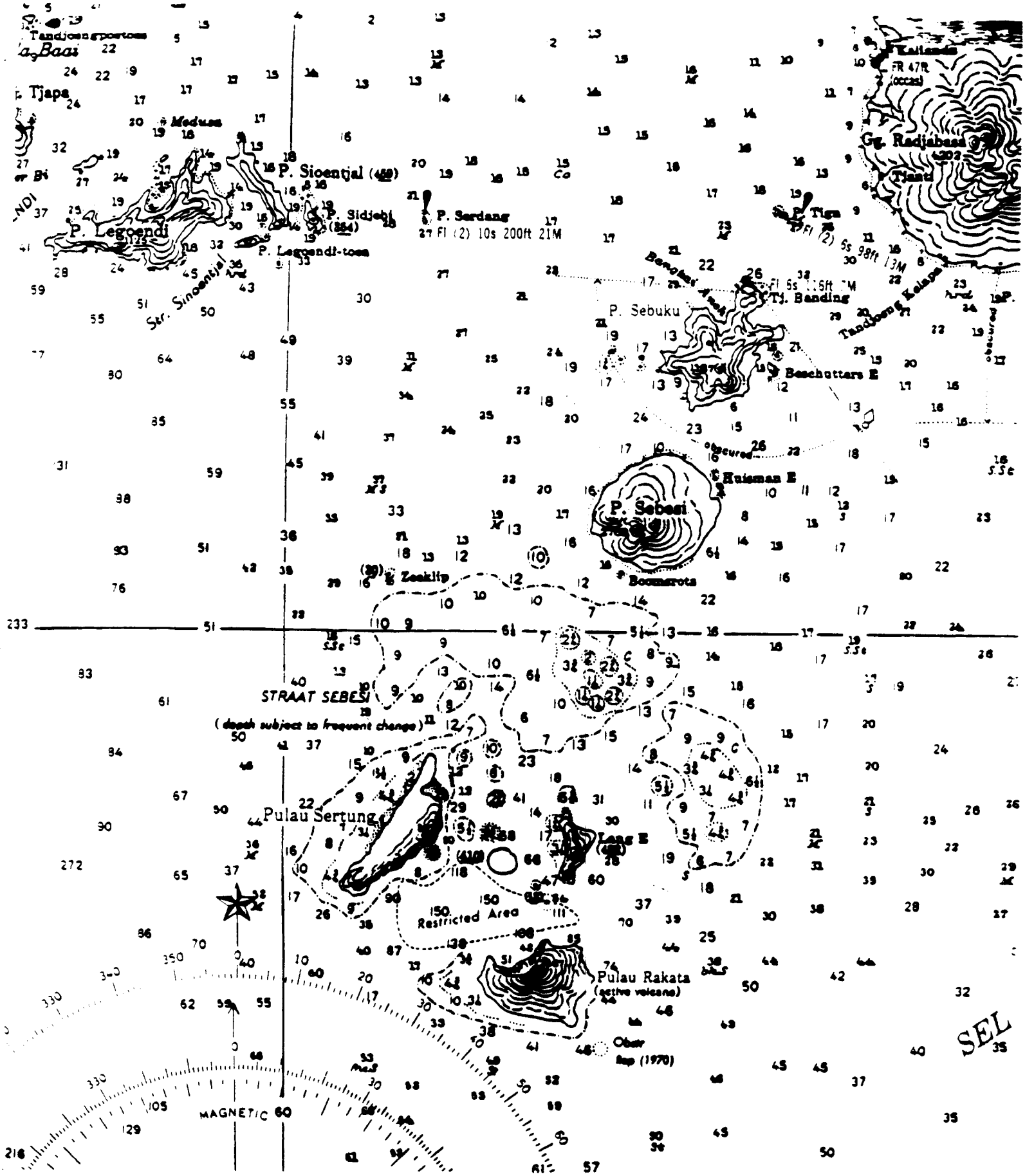

Fig. 3 Map showing the location of Legoendi, Sebesi, Sebuku and the south coast of Sumatra (Radjabasa volcano) where distal pyroclastic surge and flow deposits from the 1883 Krakatau eruption were examined in 1990.

points a few lifeless trees can be discovered" (Simkin and Fiske, 1983, p. 132). All the 150 inhabitants of Sebuku and the 80 inhabitants of Sebuku Kecil perished in the eruption. Verbeek (1885) and other visitors noted that trees were uprooted, or large tree trunks broken off at some height above the ground, "indicating violent gusts of wind". Verbeek (1885) reports that the ash deposit on Sebuku was 60 cm thick.

We found that the 1883 deposit is about 95 cm thick near sea level on Sebuku Kecil, with lithology similar to that observed on northern Sebesi. At base is a massive, pumice-bearing (4.5 cm diam.) pyroclastic flow or surge unit, overlain by a unit of rounded, well-sorted and washed pumices, capped by two pyroclastic surge and flow units on top. The succession indicates initial pyroclastic flow, followed by a major erosive event, such as a tsunami, which was in turn followed or accompanied by two pyroclastic flow and surge events.

On the northern part of Sebuku we studied the 1883 deposit along a ridge about 50 above sea level. The 51 cm thick deposit consists of three poorly-sorted and pumice-bearing (0.7 cm) pyroclastic flow deposits, but the rounded and well-sorted pumice unit observed at lower elevations on the other islands is absent. This is in keeping with the observation of Verbeek (1885) that the flood scar of the tsunami was about 30 m above sea level on Sebuku.

The island of Lagoendi is 35 km NW of Krakatau (fig. 3), and was totally devastated by the eruption, with complete loss of life. Verbeek (1885) reports that the tsunami reached about 24 m height near Lagoendi. On the northern coast we studied the 1883 deposit near sea level and on higher ground. The deposit is about 1 m thick, and divided into units similar to those observed on the other islands. At base is 15 to 26 cm massive pumice-bearing (4 cm diam.) pyroclastic flow unit, overlain by a well-sorted pumice lapilli layer consisting of reworked and rounded pumices, representing the tsunami event. This is overlain by at least two massive pyroclastic units from flow or surge activity.

Further afield, we studied the 1883 deposits on the south coast of Sumatra, around the Rajabassa volcano, about 40 km north of Krakatau (fig. 3). This area is of particular interest to the study of the eruption and its deposits, as it is here from the village of Katimbang that we have the eyewitness reports of the closest survivors of the eruption. At the time of the eruption, Controller Beyerinck was

an agent of the Dutch Colonial Government, posted in Katimbang on south Sumatra. His report and that of Mrs. Beyerinck give a dramatic and terrifying picture of the eruption from which they narrowly escaped, but which claimed the life of their youngest child.

When the Beyerincks were rescued by a search party on 1 September, five days after the eruption, their bodies were covered with burns (Simkin and Fiske, 1983). The survivors reported that "I am sure I was burnt mainly by fire that spurted out of the ground as we went along. At first, thinking only of the glowing ash showers, we endeavoured to shelter ourselves under beds, taking the risk of the house falling in, which no doubt it did on a great many, but the hot ashes came up through the crevices of the floor and burned us still more". The Beyerinck family fled the coastal village of Katimbang on the evening of 26 August, when the eruption increased in intensity and the first tsunamis threatened to wash away their house. They sought refuge in a hut on the slopes of Rajabassa volcano, at about 400 ft above sea level. During the climax of the eruption the next morning, their hut suddenly became pitch dark and ash was "being pushed up through the cracks in the floorboards like a fountain". They had been accompanied by a large number of local Sumatrans on their flight up the mountain, but the next morning about one thousand of the three thousand natives had died of burns. The ash deposit in Ketimbang was about 30 cm thick after the eruption (Verbeek, 1885).

We studied the 1883 deposit at five localities on the south Sumatra coast, at Kalianda, G. Botak, Batubalak, Rajabassa and Banding (formerly Katimbang), and found it to range from 3 to 54 cm in thickness. The deposit consists of three or four units, although some of these are clearly reworked material. Typically, the basal unit is a very poorly-sorted 3 to 10 cm thick, massive silty-sandy ash, with up to 4 cm pumice clasts. The silty matrix is often vesicular, indicating the presence of steam in the ash at the time of deposition. This unit is overlain by 12 to 24 cm of very poorly-sorted, silty-sandy ash with common coral fragments and 0.5 to 1 cm pumice clasts. This suggest that the unit is derived from deposition of the major pyroclastic surge event that invaded the Sumatra coast; the coral fragments may be derived from erosion of the off-shore coral reefs by the accompanying tsunami.

C. Pre-1883 Volcanic Succession of Krakatau Volcano

During our expedition we also had the opportunity to examine and sample deposits from eruptions which predate the 1883 event. The Krakatau volcanic complex, comprising the islands of Rakata, Panjang, Sertung and Anak Krakatau, consists of four major geologic formations (Effendi, Bronto and Sukhyar, 1986).

Krakatau Formation:

The oldest exposed rocks belong to the Krakatau Formation, and they are exposed on east Sertung, north Rakata, and south and west Panjang. The basal unit of this formation (Klat) are massive, thick and flow-banded dacitic andesite lavas (SiO_2 67.21%) on eastern Sertung island (up to 80 m thick) and on western Panjang (KRA-58, 71, 119 and 123; numbers refer to samples in our 1990 collection; see Appendix I).

The Krakatau lavas are overlain by a major pyroclastic formation, which is particularly well developed on southern Panjang island. This formation represents a major explosive event in the evolution of Krakatau volcano, and was probably associated with the early caldera formation. Lowermost unit in this formation is a dark grey to reddish brown incipiently welded dacitic scoria deposit, that is tens of meters thick locally and may have been deposited as a pyroclastic flow from a scoria cone on southern Panjang (KRA-60, 67, 115). The scoria deposit is overlain by a pinkish light grey plinian pumice fall, which reaches up to 1 m in thickness. This is in turn conformably overlain by a up to 2 m thick pumiceous pyroclastic surge sequence, which contains numerous densely welded surge lenses. The welded surge is overlain by a second plinian pumice fall layer (KRA-61, 63) and locally by up to 8 m lithic-rich pyroclastic lag deposit at south end of Panjang (KRA-59, 62). The age of this major eruption is presently unknown, but it may corelate with a silicic tephra fall layer (SiO_2 69.7%) found in a deep-sea core south of the Sunda Straits (Ninkovich, 1979). The 3 cm thick tephra in core V19-150 occurs at 222-225 cm depth sub-bottom, and has been tentatively dated about 60,000 years old.

Rakata Formation:

On Rakata island, the Krakatau formations described above are overlain by the Rakata Formation, consisting of a typical strato-cone succession of thin basaltic andesite lava flows (KRA-49), alternating with scoriaceous and tuff beds (KRA-74).

They represent the build-up of the Rakata stratocone prior to the 1883 eruption.. The Rakata Formation is cut by numerous radial dikes (KRA-76, 77) of basaltic and andesite composition.

Marine-based Studies

The vast majority of the products of the 1883 eruption were deposited in the ocean around Krakatau, and have up to now been unstudied. A primary objective of our 1990 expedition was therefore to sample and study the submarine deposits, and to compile an accurate bathymetric map of the region primarily affected by the volcanic deposition. The first phase of the marine study was an intensive bathymetric survey of the Steers and Calmeyer area north and northeast of the Krakatau island group. The purpose of this work was to produce a database to evaluate the submarine morphology of these two ephemeral islands and select locations for sample collection by SCUBA diving. Following site selection, two extended periods of diving were carried out in order to collect a suite of sediment cores and grab samples.

A. *Bathymetric Surveying of the Krakatau Region*

The 1883 eruption led to fundamental changes in the ocean floor morphology around the Krakatau islands, and detailed documentation of these changes is essential for an understanding of the volcanic processes involved. Earliest bathymetric data from the region dates back to 1881, when the *HMS Belliqueux* charted the Sunda Straits, including depth soundings north of Krakatau (Fell, 1988). This chart and the British Admiralty chart of 1875 show that the depth in the Sebesi Channel north of Krakatau was generally 20 to 30 fathoms prior to the eruption; with local deeps up to 37 fathoms just north of the Krakatau islands. We have digitized all of the existing pre-1883 bathymetric and topographic data in order to construct a contoured map of seafloor around Krakatau just prior to the eruption (fig. 4).

The first observations of the changes in the region were made by the *USS Juniata* on 10 September, 1883, two weeks after the eruption (Simkin and Fiske, 1983, fig. 32), whereas the first bathymetric survey made after the eruption was carried out by the Dutch naval survey vessel *HM Hydrograf* about one month

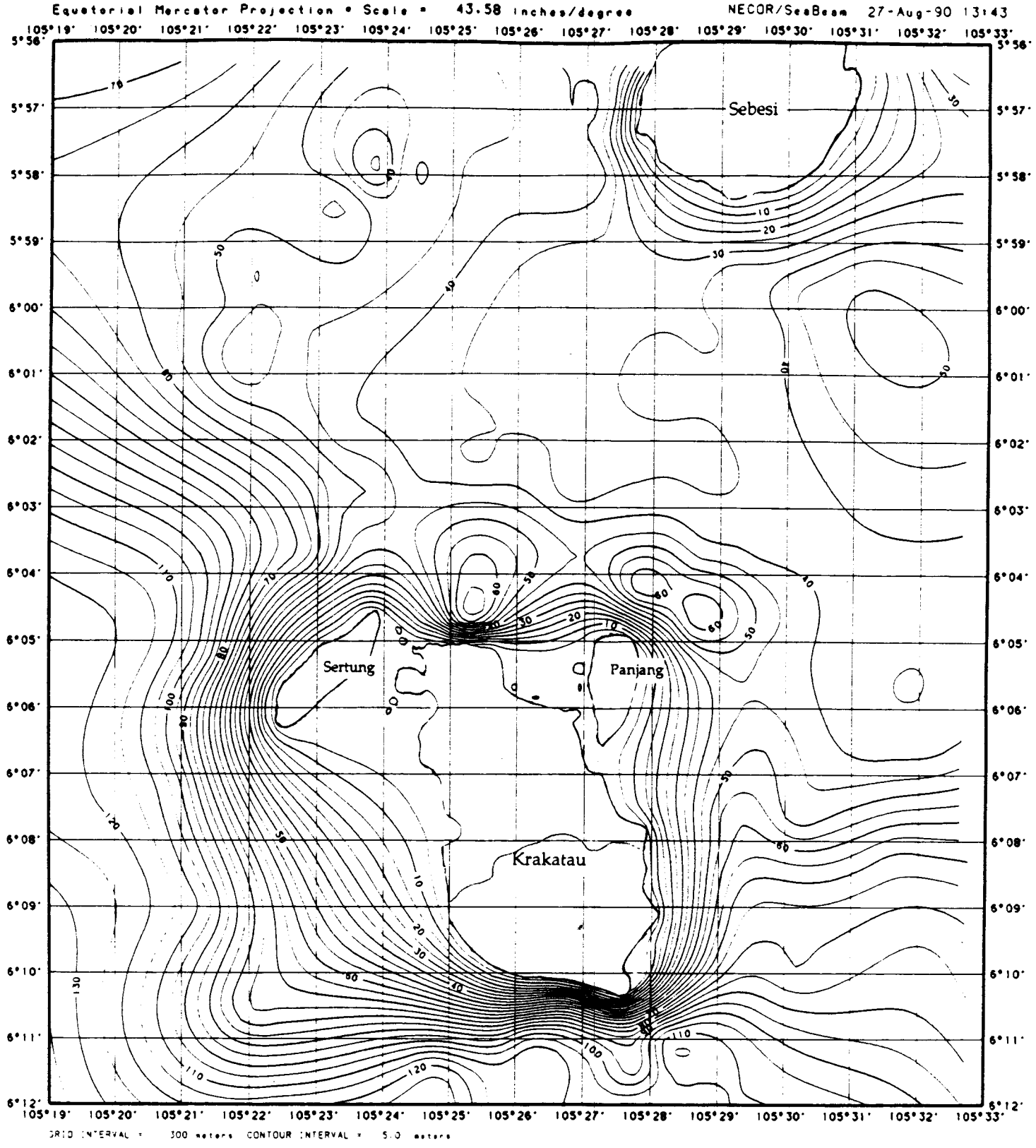

Fig. 4. Bathymetric map of the area surrounding Krakatau volcano prior to the 1883 eruption based on the survey of *H.M. Hydrograf* in October 1883. Contour intervals are in meters (see figure 4 in Verbeek, 1885).

after the event. Verbeek (1885, fig. 4) gives the most comprehensive compilation of depth soundings available before the eruption, and compares those with soundings made shortly after the eruption by the *HM Hydrograf* . On the basis of these depth changes, Verbeek proposed that about 12 km^3 of material was added to the submarine area within 15 km radius of the volcano during the eruption.

Surprisingly, there has not been a detailed survey of the seafloor around the Krakatau islands. During our expedition we carried out a new bathymetric survey of the Krakatau island group using a Raytheon recording fathometer. This instrument was satisfactory for most purposes, but due to the low power output of the transducer it was not possible to measure depths in excess of 120 m, such as within the deeper portions of the Krakatau caldera. Navigation and positioning of bathymetric profiles was primarily accomplished by use of a Trimble Transpak Satellite Navigation instrument and the GPS satellite system. SATNAV fixes were generally collected at two minute intervals during surveys. The GPS satellite "window" in the study area was about 18 hours per day. During surveys outside of the GPS "window" we obtained fixes by bearings on local landmarks, using an Autohelm Fluxgate sighting compass. Figure 5 shows the areal coverage of our 1990 survey. Continuous bathymetric data was collected along the tracklines and then sampled at 2 minute time intervals in order to develop a computer-generated bathymetric contour map (fig. 6). Because we were unable to collect information at depths greater than 120 m we have used data from Stehn (1929) to constrain the morphology of the deep caldera interior on figure 6.

The bathymetric survey was particularly useful for defining the morphology of the Steers and Calmeyer submarine platforms north and northeast of Krakatau. Examination of the continuous bathymetric records allowed us to identify a series of distinct morphological provinces including and surrounding the platforms (fig. 7). The shallow areas of the platforms (<20 m in depth) consist of a very flat bottom with small scale irregularities of less than 1 m in height. These areas likely represent the wave cut base resulting from tidal current and storm related erosion of the islands following the eruption. The outer boundaries of these area are often asssociated with steep scarps such as in the eastern part of Steers and the western part of Calmeyer (fig. 7). Moving away from the flat shallow platforms the bathymetry becomes progressively more irregular and is best described as

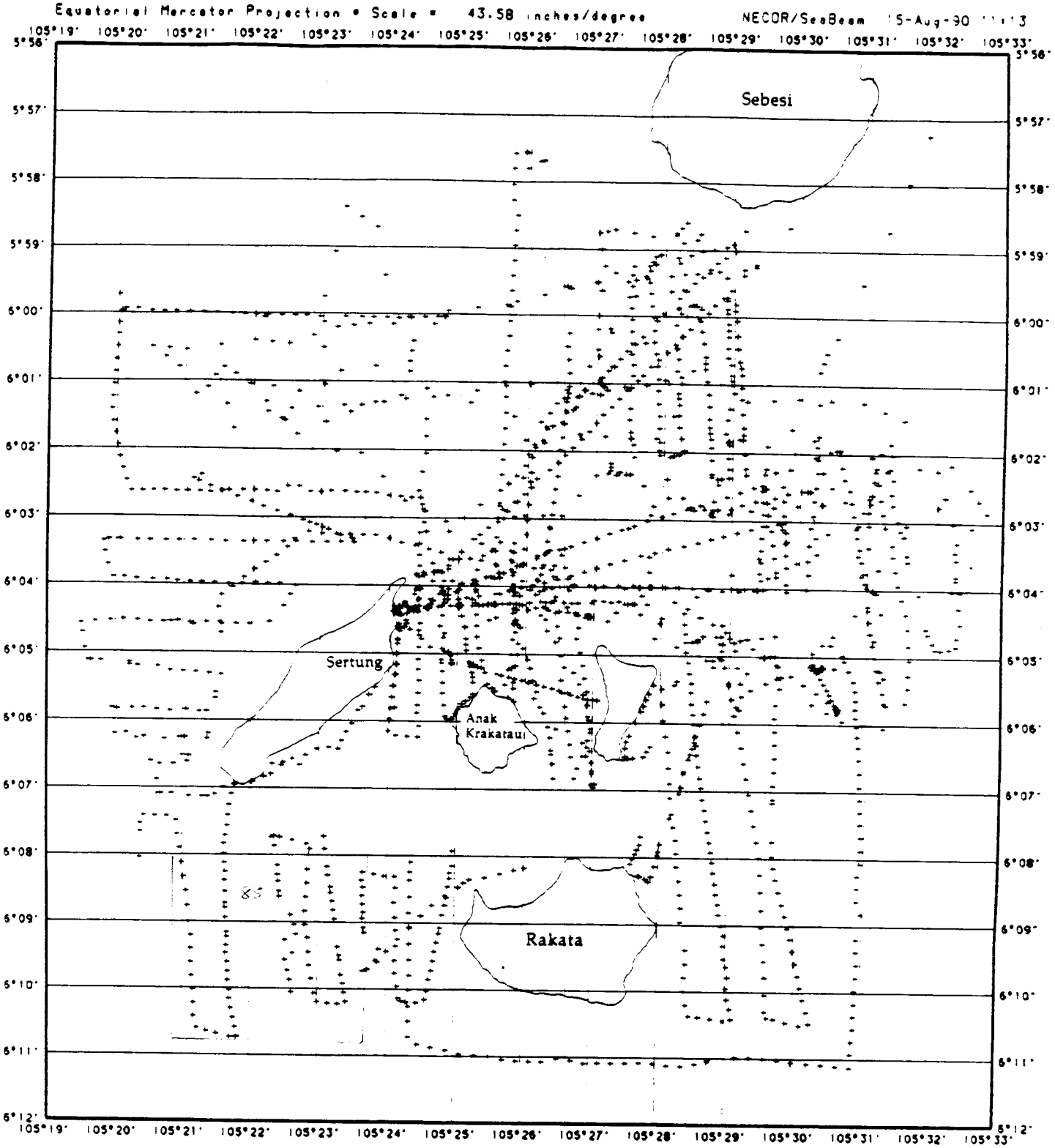

Fig. 5 Map showing the track lines of the bathymetric survey carried out during the 1990 Krakatau expedition. Plus symbols represent sampling of the continuous bathymetric profiles at 2 minute time intervals. These data were used to construct the bathymetric map shown in figure 6

hummocky. The amplitude of the hummocks increases with water depth from between 1-2 m in height to large, 6-10 m features (fig. 7). The origin of the hummocks is not yet understood but our sampling program, described below, has been able to shed new light on their lithology.

B. *Submarine Geology: Results of SCUBA Diving*

The highly destructive tsunamis that invaded the coasts of Sumatra and Java have generally been attributed to the large volume of material deposited in the Sunda Straits around Krakatau during the 1883 eruption. Ideas about the nature of the large submarine deposit and the tsunami mechanism include the following:

1. The tsunamis were generated by "cave-in" or collapse of the Krakatau volcano during caldera formation at the time of or immediately before the explosive eruption (Verbeek, 1885; Williams, 1941).

2. The tsunamis were caused by "the impact upon the water of the Strait of the enormous masses of falling material"; the short-lived islands of Steers and Calmeyer were formed as parasitic cones on the northern flank of the Krakatau volcano (Judd, 1888; Wharton, 1888).

3. Pyroclastic flows generated during the eruption swept across the floor of the Sunda Straits (Williams and McBirney, 1968; 1979), forming destructive tsunamis (Latter, 1981; Self and Rampino, 1981).

4. Debris flows formed by the northward collapse of the Krakatau volcano produced tsunamis (Camus and Vincent, 1983).

It is clear from the above, that the submarine formations deposited during the 1883 eruption should provide fundamental clues as to the nature of the erupted products and the mechanism of tsunami generation. Our aim during the 1990 Krakatau expedition was therefore to study and sample the submarine deposits as widely as possible. We designed and built a sediment coring device that could be operated by 2 SCUBA divers to obtain 7 cm diameter cores up to 1.3 m in length. Guided by our batymetric survey, we carried out 59 research SCUBA dives in the region and collected over 50 sediment cores of volcanic deposits on the ocean floor. Dives were carried out by Sigurdsson and Carey, assisted by an Indonesian professional diver, Mr. Sundjoko, who contributed greatly to the success of the

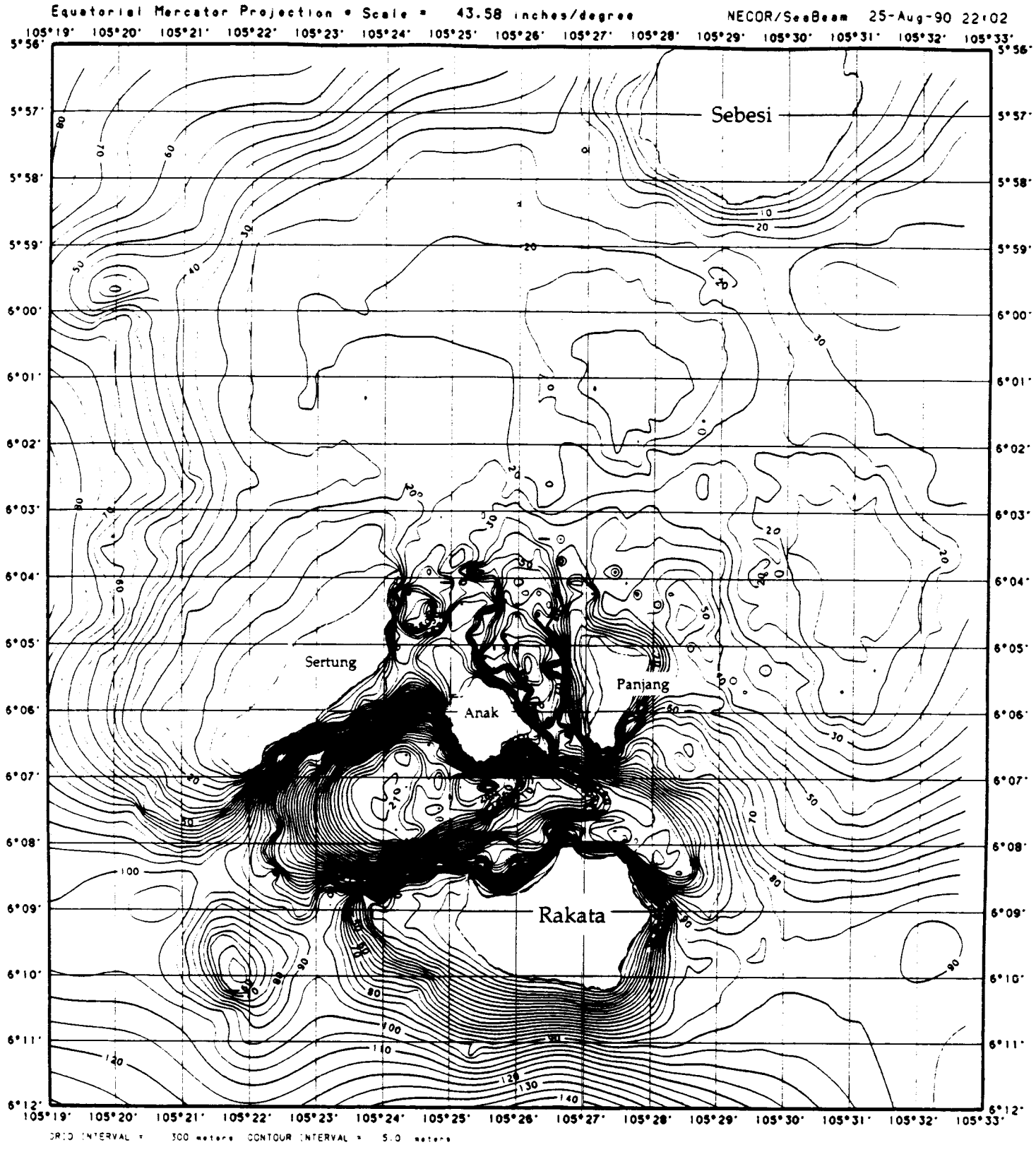

Fig. 6. Present bathymetry of the Krakatau area based on surveying work competed in 1990. Data for depths greater than 120 meters was obtained from a caldera survey in 1929 by C. Stehn.

submarine studies. On our 34th dive, Mr. Sundjoko suffered an out-of-air emergency because of a faulty air-pressure gauge and consequently inhaled some seawater. He returned to Java on the next day to have a medical checkup and made a full recovery. The remaining dives were carried out safely by Sigurdsson and Carey. Table 1 gives location, water depth and sample length of sediment cores taken during these SCUBA dives (fig. 8). The underwater study was conducted in the five areas described below:

1. The shallow-water (10 to 15 m) platform occupying the former site of Calmeyer island and adjacent area, north-east of Krakatau.

2. The shallow water platform (5 to 15 m) at the former site of Steers island and adjacent area, north of Krakatau.

3. The isolated hummocks or peaks that rise out of the relatively deep moat immediately north of the Krakatau islands.

4. The wave-cut platform west of Sertung island.

5. The shallow platforms just to the north and north-west of the active Anak Krakatau volcano.

In the majority of dives, we encountered pyroclastic flow deposit on the ocean floor, either as outcrops or draped over by a thin (5 to 15 cm) layer of reworked volcanic sands and gravel. On the shallow platforms of Steers and Calmeyer, where the 1883 deposit is up to 40 m thick, we studied the pyroclastic flow during 27 dives. At most of these sites, the deposit has an eroded surface, whereas at some sites (e.g. dives 13, 15, 18, 19, 38, 39 and 47) the sea floor may represent the primary pyroclastic flow surface, with common angular, large (20 to 70 cm) vesicular pumice clasts and large lithics (10 to 30 cm) protruding from very poorly sorted light-grey to greenish-grey pyroclastic flow matrix. There is generally considerable biological cover at these sites, and little or no sign of erosion of the primary deposit.

The principal region of pyroclastic flow deposition (Steers and Calmeyer platforms) is separated from the Krakatau volcanic complex by a moat or arcuate channel, with water depths ranging from 50 to 90 m, and there is thus indication of little or no deposition in this region during the eruption. The persistance of this channel presents a major enigma regarding the 1883 eruption. Several sharp peaks or hummocks rise out of the moat to within 10 to 15 m of sea level, and we dove

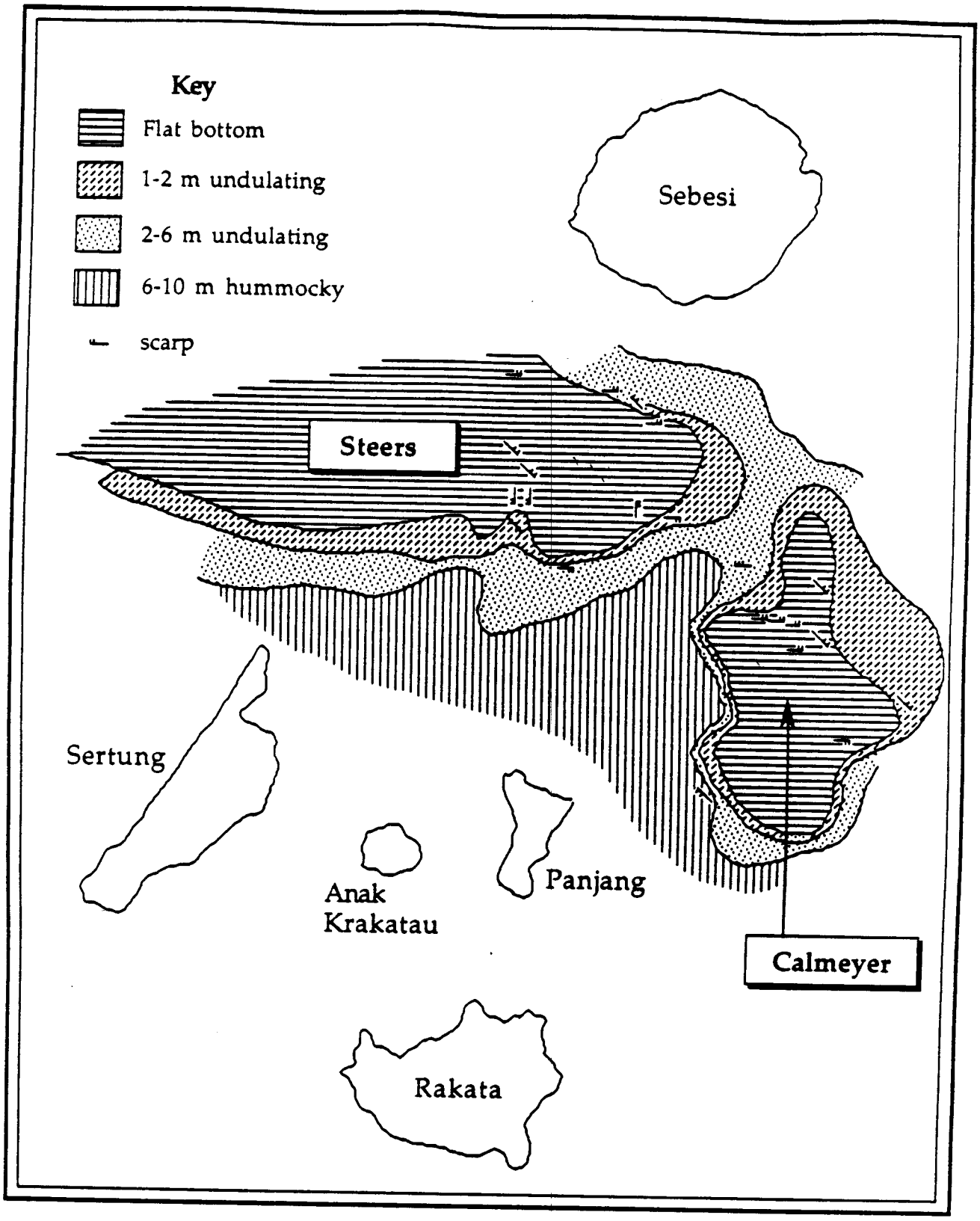

Fig. 7. Morphological facies map of the Steers and Calmeyer platform areas based on bathymetric surveying completed in 1990.

on three of these hummocks (dives 38, 39 and 52). They are composed of primary pyroclastic flow surface, with abundant angular and large (30 to 100 cm) pumice clasts and large lithics (10 to 20 cm) protruding from the surface. The pyroclastic flow deposit is grey to light-grey, poorly sorted, sandy-silty, but somewhat coarser than more distal facies of the flows seen on Steers and Calmeyer. Abundant vegetation and other biological activity indicates that erosion of these hummocks is negligible, and that they represent primary pyroclastic flow surface. Sediment cores taken in the hummocks also indicate pyroclastic flow origin.

At two shallow dive sites on the Calmeyer platform (dives 8 and 9; 46 and 47 ft) there are outcrops of a grey to light grey, well-sorted silty ash, with very fine (1 to 3 mm) sub-horizontal laminations. This deposit resembles ash fall, and we speculate that it may be a product of the phreatic explosive activity that occurred on Calmeyer and Steers islands immediately after the 1883 eruption, when the pyroclastic flow deposits were sufficiently hot to bring about steam explosions in sea water trapped under or within the flow succession, as first proposed by McLeod (1884). On 30 August, or three days after the eruption, the steamer Graaf von Bylandt observed steam explosions from Steers island (Simkin and Fiske, 1983, p. 131), and these steam explosions were still in progress on 3 September on Steers and Calmeyer islands (McLeod, 1884), but had ceased when the area was surveyed by the *USS Juniata* on 9 September (Simkin and Fiske, 1983, p.135).

The ocean floor east of Sertung is a wave-cut platform that overlies the thickest submarine deposit from the 1883 eruption, reaching up to 80 m in thickness. During three dives in this area (dives 56, 58 and 59) we studied and sampled the deposits. The surface is reworked crystal- and pumice-rich sands, with large ripple marks, indicative of the high energy on this wave-cut platform. Underlying the 10 to 30 cm reworked surface sediment, there are outcrops of pyroclastic flow, with light-grey to greenish grey silty-sandy matrix. At one site (dive 59) the pyroclastic flow contains extremely large (>1 m) angular pumice blocks and obsidian clasts in excess of 50 cm.

The surface layer of reworked volcaniclastic sediments on the Steers and Calmeyer platforms is generally sandy to gravelly, very well-sorted and dominated by crystal-rich and lithic sands and rounded light grey, vesicular pumice lapilli. In the high wave energy on the shallow (5 to 10 m) platforms, the loose surface

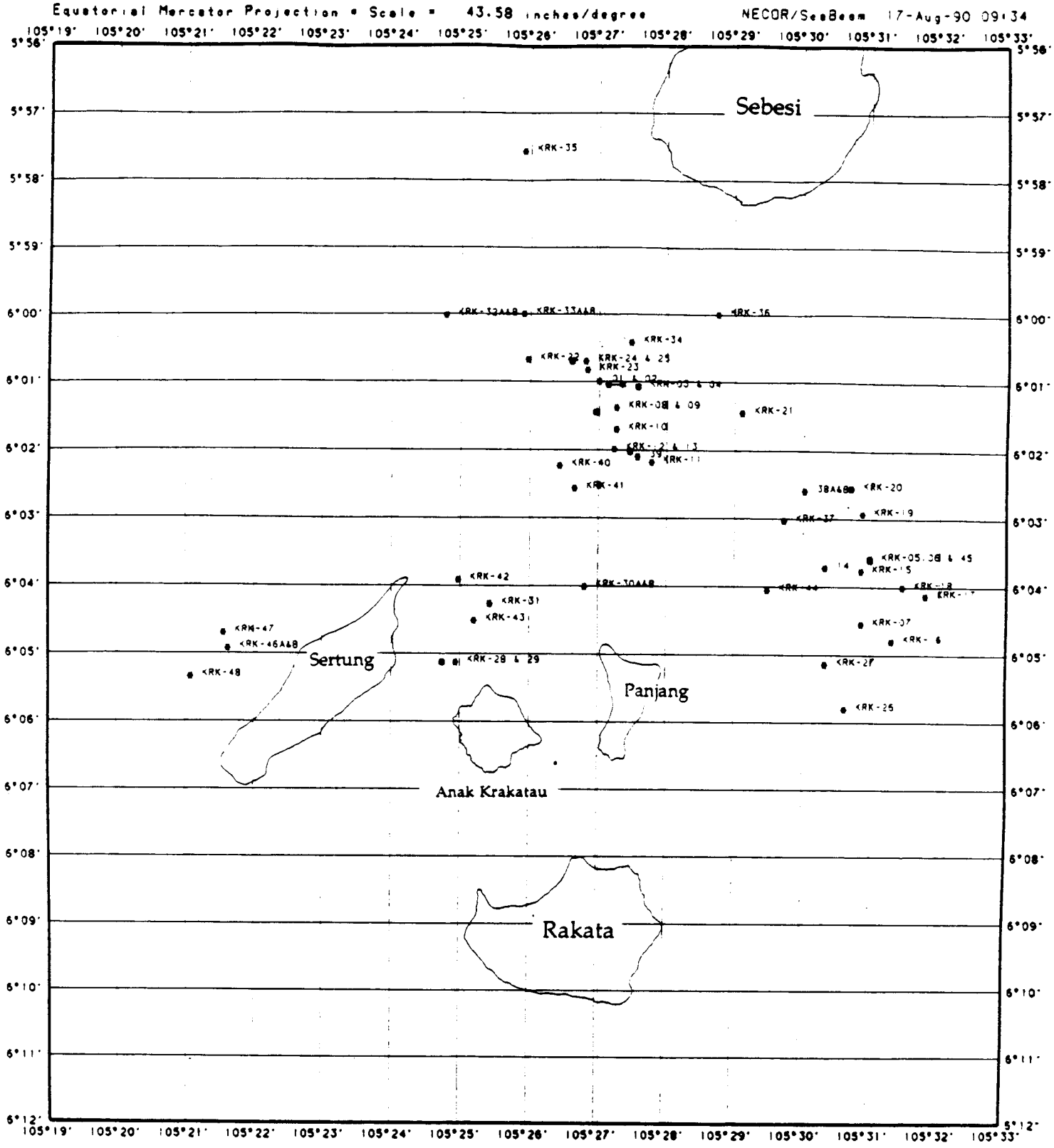

Fig. 8. Locations of sediment cores obtained by SCUBA diving during the 1990 Krakatau expedition.

sediment shows well developed ripple marks at many scales, often with wavelength of 1 m and amplitude of 10 to 40 cm. The shallowest part of the Steers platform is generally 5 to 10 m in depth, and is bounded to the west by a prominent scarp, at about middle of the Steers area. This scarp is a large dune crest, 5 to 10 m in height and with a slope of about 45^{o}, composed of crystal and pumice-rich well-sorted sands. At the western base of the dune the sea floor is dominantly composed of primary pyroclastic flow surface; thus the dune feature represents westward progradation of a sedimentary fan that is encroaching on and burying the primary pyroclastic flow surface. The source of these sediments is found in erosion of the pyroclastic flow deposit on the east margin of the Steers and Calmeyer platforms, where the eroded pyroclastic flows are exposed. The dominant westerly direction of sediment transport on the Steers and Calmeyer submarine platforms can be attributed to the very strong tidal currents in the Sunda Straits, between the Java Sea to the north and the Indian Ocean to the south.

We also explored the shallow region about 1 km NNW of Anak Krakatau volcano, during dives 36, 37 and 53. This small platform reaches within 3.5 m of the surface, but drops off very steeply to the south. The surface is composed entirely of black to dark brown poorly-vesicular tephra and sands from recent Anak Krakatau eruptions. The sands are reworked, ripple marked and in active motion. Down-slope on the steep scarp facing south (dive 53) the black Anak tephra is seen to drape over 1883 pumiceous pyroclastic flow deposit.

Conclusions

The findings and conclusions presented in this report are preliminary, as studies of sediment cores and other geologic samples, as well as data processing has just begun. A full description of the submarine pyroclastic deposits from the 1883 eruption must await the splitting of the cores, sampling, and granulometric and geochemical analysis. Preliminary results indicate, that the principal product of the 1883 eruption were pyroclastic flows, which were emplaced into the ocean around the volcano. Large accumulations occurred particularly to the west of Sertung, and in the region between the Krakatau islands and the island of Sebesi, where the

temporary islands of Steers and Calmeyer were formed as a result of the high influx of pyroclastic flows. This deposit to the north of the volcano forms a collar or shallow arcuate ridge, concentric with the volcano, but is separated from the latter by a 2 to 4 km wide moat, where depths of the order 40 to 90 m occur. Dives on peaks and hummocks in the moat region indicate that pyroclastic flow was deposited here, but its distribution is patchy and must have been very thin. The pyroclastic flow deposit on these hummocks is in all respects similar to that of the more distal deposit on Steers and Calmeyer platforms, except that pumice and lithics clasts are generally larger in the former. We found no evidence that the hummocks were composed of old lithic material from the destroyed cone of Krakatau as would be expected if the majority of the submarine deposits to the north of the volcano were generated by the hypothetical debris avalanche proposed by Camus and Vincent (1983).

The non-deposition near the volcano and formation of the moat may be related to pyroclastic flow mechanics and the density relationships between the active pyroclastic flow cloud and the underlying surface, i.e. the ocean. We envisage the eruptive mixture of pyroclastic material and associated gases as a high fountain rising above the vents or the erupting arcuate fissure of the caldera. As the fountain collapses from a height of a few km, it generates a current of pyroclastic flow that moves radially away from the volcano over the surrounding ocean. Initially, this hot density current may be less dense than the ocean and thus able to travel over water without major deposition. The flow's mobility may have been enhanced by the foramtion of a "steam cushion" at the ocean surface. Only larger clasts of lithics and pumice would be deposited as a lag layer. As the pyroclastic density flow current advances, it may increase its density due to loss of volatiles, cooling by contact with the ocean and atmosphere, and it may also increase its density by condensation of water vapor in the gas phase of the pyroclastic flow. The result of the increasing bulk density of the pyroclastic flow to a density similar to that of sea water is the entrance of the flow into the ocean water column, and deposition in the regions of Steers and Calmeyer.

It is clear, however, that a large component of the pyroclastic density current continued to flow over the ocean surface beyond Steers and Calmeyer islands, and engulfed the islands of Sebesi, Sebuku, Legondi, and reached the

Sumatra coast, over 50 km north of the volcano. We suggest, on basis of the field evidence, that this represents a relatively dilute pyroclastic surge cloud, that may have segregated from the main pyroclastic flow, and retained sufficiently low density to flow over the ocean surface.

References

Camus, G. and P. Vincent, 1983. Discussion of a new hypothesis for the Krakatau volcanic eruption in 1883. *Jour. Volc. Geotherm. Res.*, 19, 167-173.

Clausen, H. and C. Hammer, 1988. The Laki and Tambora eruptions as revealed in Greenland ice cores from 11 locations. *Annals of Glaciology*, 10, 16-22.

Devine, J., Sigurdsson, H., Davis, A., and S. Self, 1984. Estimates of sulfur and chlorine yield to the atmosphere from volcanic eruptions and potential climatic effects. *Jour. Geophys. Res.*, 89, 6309-6325.

Effendi, A.C., S. Bronto and R. Sukhyar, 1986. Geologic map of Krakatau volcano complex, Sunda Strait, Lampung Province. Volcanological Survey of Indonesia.

Fell, R.T., 1988. Early maps of South-east Asia. Oxford University Press, 103 pp.

Hammer, C., Clausen, H., and W. Dansgaard, 1980. Greenland ice sheet evidence of post-glacial volcanism and its climatic impact. *Nature*, 288, 230-235.

Jones, P., Wigley, T. and P. Kelly, 1981. Variations in surface air temperatures: part 1 Northern hemisphere, 1881-1980. *Month. Weather Rev.* , 110, 59-70.

Judd, J., 1888. On the volcanic phenomena of the eruption, and on the nature and distribtuion of the ejected materials. In: The eruption of Krakatau and subsequent phenomena, *Report of Krakatau Committee of the Royal Society*, 1888, 1-56.

LaMarche, V. and K. Hirschboeck, 1984. Frost rings in trees as records of major volcanic eruptions. *Nature*, 307, 121-126.

Latter, J.H., 1981. Tsunamis of volcanic origin: summary of causes, with particular reference to Krakatau, 1883. *Bull. Volcanol.*, 44-3, 467-490.

Ninkovich, D., 1979: Distribution, age and chemical composition of tephra layers in deep-sea sediments off western Indonesia. *J. Volcanol. Geotherm. Res.* 5, 67-86.

Papp, Z., 1983: Investigations on the climatic effects of great volcanic eruptions by the method of tree-ring analysis. Bull. Volcanol. 46-2, 89-102.

Rampino, M. amd S. Self, 1982. Historic eruptions of Tambora (1815), Krakatau (1883) and Agung (1963), their stratospheric aerosols and climatic impact. *Quat.Res.*, 18, 127-143.

Self, S. and M. Rampino, 1981. The 1883 eruption of Krakatau. *Nature*, 292, 699-704.

Sigurdsson, H., 1989. Assessment of the atmospheric impact of volcanic eruptions. *Geol. Soc. Amer. Spec. Paper,* (in press).

Simkin, T. and R. Fiske, 1983. Krakatau 1883 The volcanic eruption and its effects. Smithsonian Institution Press, Washington, D.C., 464 pp.

Stehn, C. E., 1929. The geology and volcanism of the Krakatau group. *Proc. Fourth Pacific Science Conf.*, 1-55.

Verbeek , R.D.M., 1885. Krakatau. Batavia, 495 pp.

Wexler, H., 1951: Spread of the Krakatau volcanic dust cloud as related to the high-level circulation. Bull. Am. Met. Soc. 32, 48-51.

Wharton, W., 1888. On the seismic sea waves caused by the eruption of Krakatau August 26 and 27, 1883. In: The eruption of Krakatau and subsequent phenomena, *Report of Krakatau Committee of the Royal Society,* 1888, 89-151.

Willams, H. and A. R. McBirney, 1968. An investigation of volcanic depressions: Part 1-geological and geophysical features of calderas. A progress report of work carried out under NASA research grant NGR-38-033-012, 9-10.

Willams, H. and A. R. McBirney, 1979. Volcanology. SanFrancisco: Freeman Cooper and Co., 397 pgs.

Yokoyama, I., 1981. A geophysical interpretation of the 1883 Krakatau eruption. *Jour.Volcanol. Geotherm.Res.*, 9, 359-378.

Yokoyama, I., 1987. A scenario of the 1883 Krakatau tsunami. *Jour.Volcanol.Geotherm.Res.*, 34, 123-132.

Table 1
Summary of SCUBA Dives

Dive	Lat.	Long.	Depth, ft.	Remarks
1	6° 1.026′	105° 26.927′	38	15 cm pumiceous surface layer is sandy, ripple-marked, reworked sediment. Overlies light grey, poorly sorted, silty-sandy pumice-rich pyroclastic flow deposit; 54 cm core.
2	dive at same location			same lithology as dive 1 above.
3	6° 01.0′	105° 27′	23	Over 71 cm thick sandy, pumiceous, reworked and ripple-marked surface sediment; 71 cm core.
4,5	same location as dive 3			same lithology as dive 3.
6	6° 1.076′	105° 27.562′	27	Sandy, coarse, pumiceous and reworked sediment. 47 cm core in mostly reworked volcanic sands.
7	6° 1.076′	105° 27.562′	26	Sandy to gravelly surface with up to 10 cm pumice clasts, dark grey scora and lithic clasts, reworked sediment; 109 cm core.
8	6° 3.59′	105° 30.97′	46	Thin gravelly pumice-rich surface layer, overlies silty-sandy finely laminated grey ash deposit; 59 cm core of reworked (upper) and laminated (lower) sediment.
9	6° 3.59′	105° 30.97′	47	same lithology as at dive 8 above; 7 cm core.
10	6° 4.55′	105° 30.85′	48	Gravelly, grey, pumice-rich surface sediment, some ripplemarks; 85 cm core of reworked sediments.
11	6° 1.383′	105° 27.25′	26	Reworked crystal- and pumice-rich sands, ripple-marked surface; 91 cm core.
12	6° 1.45′	105° 26.95′	44	Surface is sandy, well-sorted and crystal-rich volcanic sand, with small ripple marks; core is 115 cm, with poorly sorted, pyroclastic flow deposit in lower part.
13	6° 1.70′	105° 27.25′	44	Sandy, flat bottom, with some large (20 cm) angular pumice clasts at surface; rich biological cover; probable primary volcanic surface. Core 32 cm; upper part is reworked volcanic sands; lower part is massive, poorly sorted light grey pyroclastic flow.
14	6° 2.069′	105° 27.014′	57	Primary pyroclastic flow surface, with large (40 cm) angular pumice clasts at surface, some coral

				and other biological activity. No core.
15	6° 2.178′	105° 27.77′	63	Silty-sandy surface, with occasional large pumice clasts, abundant coral and algae. May be primary volcanic surface. Dune to the east, about 30 ft. high. Core 10 cm.
16				Exploration dive west of Panjang island.
17	6° 2.023′	105° 27.95′	27	Gravelly to sandy, pumice-rich and reworked surface, with ripplemarks; 89 cm core of reworked sands.
18	6° 1.99′	105° 27.22′	51	Primary pyroclastic flow surface, with very large (40 to 50 cm) angular pumice, dense scoria and lithics blocks; 70 cm core of poorly sorted silty-sandy pyroclastic flow, light grey, with up to 3 " pumice clasts.
19	6° 2.01′	105° 27.27′	55	Primary pyroclastic flow surface, with scattered large pumice clasts 20 to 30 cm; to the west is a sandy dune of grit-size to sandy, pumice and crystal rich volcanic sands, reworked; dune about 5 m high.
20	6° 3.723′	105° 30.312′	45	Grey, reworked sandy and gravelly bottom sediment, with rounded pumice (5-10 cm) and lithics (0.5-1 cm) and scattered large (20-30 cm) angular pumice clasts. Core 55 cm reworked gravelly sands.
21	6° 3.769′	105° 30.84′	45	Gravelly to sandy, pumice-rich surface layer, with obsidian and lithics clasts; core 89 cm has poorly sorted, light grey pyroclastic flow in lower part.
22	6° 4.80′	105° 31.30′	46	Surface layer 5 cm thick, of gravelly sands and rounded pumice and up to 15 cm lithics; overlies excellent pale greenish grey pyroclastic flow outcrop, very poorly sorted, with 10 cm angular vesicular pumice clasts; silty matrix.
23	6° 4.134′	105° 31.79′	49	Five cm thick gravelly pumice-rich surface layer, with some up to 40 cm angular pumice clasts scattered; overlies light grey pyroclastic flow outcrop with 15 cm angular pumice clasts in silty matrix; 81 cm core of pyroclastic flow.
24	6° 4.005′	105° 31.45′	51	Gravelly, pumice-rich surface layer, overlies massive and coarse pyroclastic flow outcrop, light grey, silty matrix, with large, angular and vesicular pumice clasts; core 89 cm of pyroclastic flow.

25	6° 2.93′	105° 30.86′	47	Sandy to gravelly pumice-rich surface sediment with 0.5 cm lithics and 30 cm pumice clasts; core 95 cm of reworked sands.
26	6° 2.55′	105° 30.70′	60	Gravelly surface layer of very coarse pumice clasts, 30 to 40 cm apart, reworked sands. Core 67 cm of reworked gravelly volcanic sands, with lowermost part of poorly-sorted sandy-silty sediment; possible pyroclastic flow.
27	6° 1.45′	105° 29.10′	52	Sandy to gravelly surface layer, with abundant carbonate fragments of molluscs, corals and common rounded pumice and small lithics. Core 86 cm, with reworked upper part; silty-sandy pyroclastic flow in lower part.
28			20	
29	6° 0.68′	105° 25.96′	65	Silty, yellowish grey surface, with burrows of fish; core 33 cm of poorly sorted silty-sandy pyroclastic sediment ?
30	6° 0.831′	105° 26.825′	78	Sandy, scoured surface, reworked, with scattered large pumice clasts (20 cm); core 78 cm with upper reworked sands, lower part of poorly sorted light grey, silty-sandy pyroclastic flow.
31	6° 0.70′	105° 26.60′	34	Sandy-gravelly, lithic-rich surface layer 10 cm thick, underlain by light grey pyroclastic flow outcrop, poorly sorted, silty-sandy matrix; core 78 cm long.
32	6° 0.70′	105° 26.80′	31	Sand dune east of dive 31; consists of very well sorted crystal sands, with pumice-rich lenses in troughs between ripple crests.
33	6° 5.776′	105° 30.587′	62	Coarse pumice gravel at surface, very active erosion of bottom, large-wavelength ripples; core 85 cm of reworked sands and gravel.
34	6° 5.144′	105° 30.323′	62	A narrow crest, with an outcrop of grey pyroclastic flow; large (1 m) angular pumice blocs and dense lithics (50 cm) scattered at surface; pyroclastic flow is very lithic-rich, with light grey silty matrix, poorly sorted.
35	6° 5.144′	105° 30.323′	66	Same site as dive 34 above. Exceptionally coarse surface clasts and unusually abundant lithics.
36	6° 5.13′	105° 24.93′	21	Black to dark grey Anak Krakatau sands and lapilli, well sorted, ripple-marked and reworked sediments.

37	6° 5.13′	105° 24.73′	65	Black Anak sands in upper part, but lower part of steep south-facing slope (>36 ft) consists of angular, light grey large pumice clasts and lithics in sandy matrix.
38	6° 4.01′	105° 26.795′	38	Surface layer of large (30-50 cm) angular pumice clasts and lithics (10-20 cm); abundant vegetation and biological activity, little or no erosion of primary pyroclastic flow surface. Under 5 to 10 cm gravelly surface layer there is pyroclastic flow outcrop, very pumice-rich, sandy-silty matrix; core 55 cm.
39	6° 4.269′	105° 25.423′	35	Primary pyroclastic flow surface, with no sign of erosion; covered by large (50-100 cm) angular pumice blocks with abundant growth. Outcrop of pyroclastic flow is sandy-silty light grey, with abundant angular pumice and lithics clasts; core 50 cm long.
40	6° 0.041′	105° 24.791′	61	Brownish grey, sandy surface with small ripples in 10 cm thick surface layer. Underlain by light grey sandy-silty pyroclastic flow with pumice clasts; core 76 cm.
41	6° 0.00′	105° 25.90′	55	Brownish grey, sandy surface with small ripple marks and numerous 1 m diameter and 30 cm deep burrows or pits. Under 10 cm thick surface layer of reworked sediment there is outcrop of pyroclastic flow, light grey, poorly sorted, pumice-rich, with sandy-silty matrix which is lithic-rich; core 65 cm.
42	6° 0.421′	105° 27.465′	32	Yellowish grey, vegetated bottom, with lithic-rich gravelly sands and abundant 30-40 cm angular pumice clasts and lithics. Under 5-15 cm surface gravel there is pyroclastic flow outcrop, indurated, with lithology varying from matrix-dominated, silty deposit, to pumice-domnated pyroclastic flow; also lithic-rich lenses.
43	6° 0.421′	105° 27.465′	32	Same location as dive 42; pyroclastic flow very lithic-rich, with common 1-4 cm lithic clasts, up to 10 cm; pumices up to 40 cm.
44	5° 57.554′	105° 25.878′	69	Hummock with brownish grey surface and well-developed ripples in sandy, crystal-rich and pumiceous sediment. Core 72 cm of reworked volcanic sands.

45	6° 0.00′	105° 28.75′	58	Greyish-brown surface sediment with abundant vegetation and angular 10-40 cm pumice clasts and some lithics. Under 5 cm gravelly surface layer there is pyroclastic flow outcrop, indurated, with light-grey indurated silty matrix, and up to 15 cm angular pumice and 3-5 cm angular lithics.
46	6° 3.033′	105° 29.712′	56	Surface sediment of light grey, reworked sandy, pumice-rich gravel; core 38 cm.
47	6° 2.596′	105° 30.009′	59	Probable primary pyroclastic flow surface, with 30 cm angular pumice clasts protruding; common vegetation, little or no sign of recent erosion; numerous 1 m diameter circular pits at surface. Under gravelly surface patches there is primary pyrocalstic flow, light grey, silty matix, with 5-10 cm angular pumice clasts; 60 cm core.
48	6° 2.098′	105° 27.562′	30	Sandy, reworked sediment, large dune crest, with megaripples on lee side; crystal-rich sand and rounded pumice lapilli; 42 cm core of reworked sediment.
49	6° 3.22′	105° 25.17′	32	Dive aborted.
50	6° 2.237′	105° 26.469′	49	Greyish-brown surface, with abundant angular large (40 cm) pumices and lithics (35 cm), vegetation abundant; possible primary pyroclastic flow surface; outcrops of silty-sandy, light-grey pyroclastic flow, pumice-rich.
51	6° 2.568′	105° 26.643′	60	Brownish-grey surface layer of gravelly sediment, with 20-40 cm angular pumice and 30 cm lithics; abundant vegetation; fish burrows or pits up to 1m. Pyroclastic flow under reworked surface layer, matrix-rich, light grey, pumice-rich; lithics are abundant; core 49 cm.
52	6° 3.917′	105° 24.965′	54	Large coral heads, abundant algae and sponges at surface. Under 30 cm carbonate gravel and sand layer, there is pyroclastic flwo outcrop, pumice-rich; core 54 cm.
53	6° 4.516′	105° 25.195′	31	Dark grey to black sandy lapilli from Anak Krakatau. Ripple marks trhoughout the reworked surface; 70 cm core.
54	6° 4.055′	105° 29.475′	58	Yellowish brown, sandy to gravelly surface, with scattered angular pumice clasts up to 35 cm. Under thin surface layer there is silty-sandy, light-grey pyroclastic flow deposit; core 41 cm.

55	6° 3.603′	105° 30.972′	45	Brownish grey gravelly to sandy 10 to 15 cm surface layer, with abundant large (30 cm) pumice clasts and angular 10 cm lithics. Under gravel there is light-grey, pumce-rich pyroclastic flow outcrop; core 30 cm.
56	6° 4.932′	105° 21.618′	49	Patches of reworked, gravelly to crystal-rich sandy and ripple-marked sediment, overlie silty-sandy, stratified and poorly sorted deposit of possible pyroclastic flow origin; core 63 cm.
57			19	Dive north of Panjang, on reefs for exploration and photography.
58	6° 4.705′	105° 21.553′	56	Light-grey, sandy surface, ripple-marked, reworked sediment. Underlain by light-grey, massive, silty-sandy pumice-bearing pyroclastic flow deposit; core 84 cm.
59	6° 5.35′	105° 21.073′	55	Light-grey surface, with large sand ripples in crystal-rich sands, reworked. Underlain by pyroclastic flow deposit, that outcrops in places and contains 1 m angular pumice clasts and 50 cm obsidian clasts; core 75 cm long.

Appendix I: List of Geologic Samples

KRA-01: Bulk sample of crystal-rich sand from dune crest, 30 ft. depth, dive 15, Steers region; 6° 2.178′ and 105° 27.77′

KRA-02: Large rounded pumice clast from bottom in Steers region, dive 17, 27 ft; 6° 2.023′ and 105° 27.95′.

KRA-03: Lithic block form sediment surface collected on sea floor in Steers region during dive 18; location 6° 1.99′ and 105° 27.22′ and depth 51 ft.

KRA-04: Light grey vesicular pumice clast, 14 cm diameter, sub-rounded; from pumice concentration zone at base of sand dune at 6° 2.01′ and 105° 27.27′ in Steers region; depth 55 ft.

KRA-05: Light grey, poorly vesicular and angular pumice clast from sandy plain with scattered pumices, west of the sand dune at 6° 2.01′ and 105° 27.27′ in Steers region; depth 55 ft.

KRA-07: Obsidian clast with pumiceous, highly vesicular margin; dive 21, Calmeyer region, 6° 3.769′ and 105° 30. 84′, depth 45 ft.

KRA-08: Large pumice clast 20 cm diam.; dive 21, Calmeyer region, 6° 3.769′ and 105° 30. 84′, depth 45 ft.

KRA-09: Bulk sample of pumice and pyroclastic flow matrix from pyroclastic flow outcrop on sea floor, dive 22, 46 ft. 6° 4.8′ and 105° 31.3′.

KRA-10: Lithic clasts from pyroclastic flow outcrop on sea floor, dive 22, 46 ft. 6° 4.8′ and 105° 31.3′.

KRA-11: Pumice clast from sediment surface, Calmeyer region, dive 23, at 6° 4.134′ and 105° 31.79′ at depth of 49 ft.

KRA-12: Pumice clast from sediment surface at 51 ft. depth, Calmeyer region, dive 24, at 6° 4.005′ and 105° 31.45′.

KRA-13: Pumice and lithics clasts from sediment surface in Calmeyer region, dive 25, depth 47 ft. at 6° 2.93′ and 105° 30.86′

KRA-14: Two pumice clasts and a lithic from sediment surface in Calmeyer region, dive 26, depth 60 ft. at 6° 2.55′ and 105° 30.70′

KRA-15: A quarter of a very large pumice clast from sediment surface in Calmeyer region, dive 26, depth 60 ft. at 6° 2.55′ and 105° 30.70′

KRA-16: Large pumice clast (20 cm) from bottom surface in Steers region, depth 41 ft. at 6° 0.831′and 105° 26.825′

KRA-17: Lithics and pumice clasts from surface sediment, dive 31, depth 34 ft. at 6° 0.7′ and 105° 26.6′, Steers region.

KRA-18: Bulk sample of pyroclastic flow outcrop on sea floor, dive 31, depth 34 ft.

a t

6^{o} 0.7′ and 105^{o} 26.6′, Steers region.
KRA-19: Basaltic andesite lava flow from Anak Krakatau, Ala 2 (1973?).
KRA-20: Basaltic andesite lava flow from Anak Krakatau, Ala 3 (1972/1973).
KRA-21: Basaltic lava flow from Anak Krakatau, Alb (1980?).
KRA-22: Basaltic andesite lava flow from Anak Krakatau, 1988 flow.
KRA-23: Andesite lava flow from Anak Krakatau, 1963 flow.
KRA-24: Basaltic andesite lava flow from Anak Krakatau, Ala 3 (1972/1973).
KRA-25: Basaltic andesite lava flow from Anak Krakatau, Ala 4 (1975).
KRA-26: Basaltic andesite lava flow from Anak Krakatau, Ala 3 (1972/1973).
KRA-27: Basaltic andesite lava flow from Anak Krakatau, Alab (1979).
KRA-29: Bulk sample of pyroclastic flow deposit on eastern slope of Rakata island, 200 m above sea level, on summit trail; 6^{o} 9′ and 105^{o} 27.5′
KRA-30: Basaltic lava flow of Rakata formation, east coast of Rakata; forms basement to 1883 pyroclastic succession; 6^{o} 9′ and 105^{o} 27.7′
KRA-31: Charcoal from plinian layer 7 in 1883 pyroclastic succession on east coast of Rakata island.
KRA-32: Largest lithic clasts in layer 7, 1883 pyroclastic deposits, Eeast coast of Rakata; 6^{o} 9′ and 105^{o} 27.7′
KRA-33: Largest pumice clasts in layer 7, 1883 pyroclastic deposits, Eeast coast of Rakata; 6^{o} 9′ and 105^{o} 27.7′
KRA-34: Largest lithics clasts in pumice fall layer 16 in 1883 pyroclastic succession on east coast of Rakata.
KRA-35: Largest pumice clasts in pumice fall layer 16 in 1883 pyroclastic succession on east coast of Rakata.
KRA-36: Pumice clasts from layer 4 plinian pumice fall deposit of 1883 eruption, locality on beach on east coast of Rakata island, at anchorage.
KRA-36: Pumice from Rakata beach.
KRA-37: Banded xenoliths from the surface of the youngest Anak Krakatau pyroclastic cone.
KRA-38: Flow-banded andesitic lava flow, basement to 1883 pyroclastic succession on east coast of Sertung, about 500 m south of Forestry station.
KRA-40: Scoria clast from coarsest and lowermost exposed layer (1) of the "Danan" formation, east coast of Sertung island.
KRA-41: Lava flow at sea level, east coast of Sertung.
KRA-42: Diorite block from beach, east coast of Sertung.
KRA-43: Bulk sample of 48 cm thick sandy-silty ash deposit, layer 3 in 1883 pyroclastic succession on east coast of Sertung.
KRA-44: Obsidian clast from 6 m thick 1883 pyroclastic flow deposit, south-east coast of Sertung.
KRA-45: Obsidian-pumice clast from basal pyroclastic flow deposit, 1883 succession, south-east Sertung island.
KRA-46: Bulk sample of lowermost 1883 pyroclastic flow deposit, south-east coast of Sertung island.

KRA-47: Sample of 1 m long pale grey pumice clast in lower part of 1883 pyroclastic flow, south-east Sertung island.
KRA-48: Bulk sample of layer 2 in 1883 pyroclastic succession, Island Point, west coast of Rakata; 22 cm olive grey silty ash with accretionary lapilli.
KRA-49: Basaltic andesite lava flow of Rakata lava formation, underlies 3 m scoria deposit, south of Island Point, west Rakata.
KRA-50: Largest lithic and pumice clasts from layer 5 fall deposit, 1883 succession, Island Point, west Rakata
KRA-51: Largest lithic and pumice clasts from layer 7 fall deposit, 1883 succession, Island Point, west Rakata.
KRA-52: Largest lithic and pumice clasts, layer 11 of 1883 pyroclastic succession, Island Point , west Rakata.
KRA-53: Mafic pumice clasts from basal part of 1883 pyroclastic flow deposit, west coast of Rakata, 500 m north of Island Point.
KRA-54: Lithic clasts from lithic-rich pyroclastic deposit, basal part of 1883 succession, west coast of Panjang island.
KRA-55: Pumice clasts from lithic-rich pyroclastic deposit, basdal part of 1883 succession, west coast of Panjang island.
KRA-56: Pumice clasts from pyroclastic flow deposit overlying the 1883 lithic-rich pyrolcastic deposit, west coast of Panjang island.
KRA-57: Diorite block from breccia layer, that rests on top of pre-1883 lava flow, and is overlain by 1883 pyroclastic flow deposit, south-west coast of Panjang island.
KRA-58: Flow-banded and vesicular andesitic lava flow, which underlies breccia in KRA-57, south-west coast of Panjang island.
KRA-59: Pumice and obsidian clasts from pumice fall deposit on top of the scoria cone, south-east point of Panjang island; pre-1883 succession.
KRA-60: Scoria clast form lowermost exposed part of basal scoria cone, south-east point of Panjang island.
KRA-61: Pumice and obsidian clasts from second pumice fall layer, south-east point of Panjang island.
KRA-62: Pumice clasts from lithic-breccia deposit, south-east point of Panjang island.
KRA-63: Lithick clasts from upper pumice fall on south-east point of Panjang island (same deposit as sample KRA-61).
KRA-64: Bulk sample of 2.5 cm thick olive silty ash layer 2, 1883 succession on south point of Panjang island.
KRA-65: Bulk sample of 3 cm sandy-silty ash layer 1A in 1883 succession, south point of Panjang island.
KRA-66: Largest clasts of pumice and lithics, layer 3 of 1883 pyroclastic succession, south point of Panjang island.
KRA-67: Mafic pumice from top of welded scoria deposit, west coast of Panjang island (layer 1).
KRA-68: Bulk sample of basal part of 1883 pyroclastic flow deposit, west coast of Panjang (layer 4).
KRA-69: Bulk sample of layer 5, an 18 cm pumice lapilli deposit in 1883

succession, west coast of Panjang.
KRA-70: Bulk sample of layer 7 in 1883 pyroclastic succession, west coast of Panjang.
KRA-71: Flow-banded andesitic lava flow, south-west coast of Panjang island. Krakatau formation of Effendi et al. (1986).
KRA-72: Pumice clasts, layer 5 of pre-1883 pyroclastic succession; 33 cm pumice fall, Black Point, west Rakata.
KRA-73: Scoria clasts from layer 9 of the pre-1883 pyroclastic succession, Black Point, west Rakata.
KRA-74: Scoria from massive brown tuff unit 1 in Rakata cliff section.
KRA-75: Welded tuff unit 5 in Rakata cliff section; columnar jointed.
KRA-76: The large dike, Rakata cliff section.
KRA-77: Basaltic dike, 50 cm thick, cutting units 5 to 8, Rakata cliff section.
KRA-78: Densely welded tuff from unit 8, Rakata cliff section.
KRA-79: Basaltic lava flow, Huismans Island, east of Sebesi.
KRA-80: Soil sample from surface of Husimans Island, east of Sebesi.
KRA-81: Bulk sample, layer 2, excavation in plantation, 1 km SW of Segemom village, north Sebesi.
KRA-82: Bulk sample, layer 3 of 1883 deposit, excavation in plantation, 1 km SW of Segemom village, north Sebesi.
KRA-83: Bulk sample, layer 4, excavation in plantation, 1 km SW of Segemom village, north Sebesi.
KRA-84: Bulk sample, layer 5, excavation in plantation, 1 km SW of Segemom village, north Sebesi.
KRA-85: Bulk sample, layer 6, excavation in plantation, 1 km SW of Segemom village, north Sebesi.
KRA-86: Bulk sample, layer 7, lower part, excavation in plantation, 1 km SW of Segemom village, north Sebesi.
KRA-87: Bulk sample, layer 7, upper part, excavation in plantation, 1 km SW of Segemom village, north Sebesi.
KRA-88: Bulk sample, layer 8, excavation in plantation, 1 km SW of Segemom village, north Sebesi.
KRA-89: Bulk sample, layer 2, 34 cm thick, from 1883 deposit on Sebuku Kecil island.
KRA-90: Layer 3, from 1883 deposit, 13 cm pumice lapilli, Sebuku Kecil island.
KRA-91: Layer 4 from 1883 deposit, Sebuku Kecil island.
KRA-92: Basaltic andesite clasts from pre-1883 breccia, Sebuku Kecil island.
KRA-93: Bulk sample of layer 2, 1883 pyroclastic deposit, outcrop on north side of river bank, near copra factory, Tejang village, east Sebesi.
KRA-94: Bulk sample of layer 3, 1883 pyroclastic deposit, Tejang village, east Sebesi.
KRA-95: Bulk sample of layer 4, 1883 pyroclastic deposit, Tejang village, east Sebesi.
KRA-96: Bulk sample of layer 5, 1883 pyroclastic deposit, Tejang village, east Sebesi.
KRA-97: Bulk sample of layer 6, 1883 pyroclastic deposit, Tejang village, east Sebesi.
KRA-98: Layer 2 bulk sample, Leganada village, south-east Sebesi.
KRA-99: Layer 3, bulk sample, Leganada village, south-east Sebesi.

KRA-100: Bulk sample of layer 3, in 1883 pyroclastic deposit; hole dug in plantation at 90 m above sea level, about 2 km west of Leganada village, south-east Sebesi.
KRA-101: Bulk sample of layer 4, in 1883 pyroclastic deposit; hole dug in plantation at 90 m above sea level, about 2 km west of Leganada village, south-east Sebesi.
KRA-102: Bulk sample of pinkish grey ash layer 2, 1883 deposit on ridge south of Teluk Berak bay, Sebuku island.
KRA-103: Bulk sample of ash layer 3, 1883 deposit on ridge south of Teluk Berak bay, Sebuku island.
KRA-104: Bulk sample of layer 2, 1883 pyrolcastic deposit in soil section near beach west of Kalianda, south Sumatra.
KRA-105: Sample of layer 2 of 1883 pyroclastic deposit, soil section near beach, 6 km south-east of Candi, near G. Botak, south Sumatra.
KRA-106: Sample of silty massive ash layer 2, 1883 deposit, soil section near beach, 6 km south-east of Candi, near G. Botak, south Sumatra.
KRA-107: Bulk sample of pumice layer 5, 1883 deposit, soil section near beach, 6 km south-east of Candi, near G. Botak, south Sumatra.
KRA-108: Bulk sample of layer 3, 1883 deposit in Rajabassa village, south Sumatra.
KRA-109A: Bulk sample of layer 3, 1883 pyroclastic deposit, Banding village, river bank north of village, south Sumatra.
KRA-109B: Basaltic clast, breccia deposit, Legondi island.
KRA-110: Layer 2, 1883 pyroclastic deposit on Legondi island.
KRA-111: Layer 3, 1883 pyroclastic deposit on Legondi island.
KRA-112: Layer 4, 1883 pyroclastic deposit on Legondi island.
KRA-113: Bulk sample of 1883 pyroclastic flow deposit, Legondi island.
KRA-114: Pumice and lithics clasts, from 80 cm fall deposit of pre-1883 succession, Shark Cove, east Rakata island.
KRA-115: Scoria deposit underlying the 1883 pyroclastic succession, Shark Cove, east Rakata.
KRA-116: Largest clasts, layer 4, 1883 pyroclastic succession, Shark Cove, east Rakata.
KRA-117: Largest clasts, layer 10, 1883 pyroclastic succession, Shark Cove, east Rakata.
KRA-118: Largest clasts, layer 6, 1883 pyroclastic succession, Shark Cove, east Rakata.
KRA-119: Tridymite-andesite lava flow, at sea level in Shark Cove, east Rakata.
KRA-120: Pumice clasts from layer 1, lithic-rich pyroclastic breccia, east Panjang island.
KRA-121: Charcoal from pumice layer near base of exposed succession of 1883 deposits, east Panjang island (layer 4).
KRA-122: Banded pumice clast from layer 11 of 1883 pyroclastic deposit, east Panjang island.
KRA-123: Lava flow underlying the welded pumice and scoria succession, east Panjang island.
KRA-124: Banded pumice clasts from lower coarse stratified "flow" deposit (layer 0) in 1883 succession, north-west Panjang island.

KRA-125: Layer 3 silty-sandy ash deposit, 1883 succession, north end of Panjang island.
KRA-126: Layer 4, 34 cm thick olive grey ash deposit, 1883 succession, north end of Panjang island.
KRA-127: Banded pumice from 1883 pyroclastic flow deposit, layer 2 at locality on top of cliff section, wet Panjang island. May be top-most or youngest pyroclastic flow in the 1883 succession.
KRA-128: Bulk sample of matrix of lithic-rich layer 2, cliff section above the Valley of the Pumice People, west Panjang island.
KRA-129: Bulk sample of lithic-poor pyroclastic flow layer 4, cliff section above the Valley of the Pumice People, west Panjang island.
KRA-130: Charcoal from layer 2, possible pre-1883 soil layer at south-west part of Panjang island.
KRA-131: Pumice clasts from layer 2, possible pre-1883 soil layer at south-west part of Panjang island.
KRA-132: Scoria from layer 1, pyroclastic succession, south-east point of Anak Krakatau island. Dark grey scoria fall deposit.
KRA-133: Part of 40 cm dark scoria clast from layer 6 scorial fall, pyroclastic succession, south-east point of Anak Krakatau island.
KRA-134: Lighter gray, vesicular scoria clast from layer 6 scorial fall, pyroclastic succession, south-east point of Anak Krakatau island.
KRA-136: Largest clasts in layer 3, 11 cm pumice fall, 1883 succession, at outcrop on east coast of Sertung island, about 500 m south of Forestry station.
KRA-137: Largest clasts of pumice and lithics from layer 5, 1883 succession, at outcrop on east coast of Sertung island, about 500 m south of Forestry station.
KRA-138: Largest clasts of pumice and lithics from layer 6, 1883 succession, at outcrop on east coast of Sertung island, about 500 m south of Forestry station.
KRA-139: Bulk sample of layer 6, 1883 succession, at outcrop on east coast of Sertung island, about 500 m south of Forestry station.
KRA-140: Obsidian breccia from 1883 pyroclastic flow deposit exposed along the middle of west coast of Sertung island.
KRA-141: Bulk sample of matrix of 1883 pyroclastic flow exposed along the middle of west coast of Sertung island.
KRA-142: Bulk sample of 1883 pyroclastic flow matrix exposed along the middle of west coast of Sertung island.
KRA-151: Obsidian block from Sertung 1883 pyroclastic flow deposit.

Appendix II: List of Sediment Cores

Core No.	Latitude	Longitude	Water Depth (ft)	Length (cm)
KRK-01	6° 1.044′	105° 27.128′	38	54
KRK-02	6° 1.000′	105° 27.00′	23	71
KRK-03	6° 1.075′	105° 27.562′	27	47
KRK-04	6° 1.076′	105° 27.562′	26	109
KRK-05	6° 3.590′	105° 30.970′	40	58
KRK-06	6° 3.590′	105° 30.970′	40	7
KRK-07	6° 4.550′	105° 30.850′	48	85
KRK-08	6° 1.383′	105° 27.250′	26	91
KRK-09	6° 1.450′	105° 26.950′	44	115
KRK-10	6° 1.700′	105° 27.250′	44	32
KRK-11	6° 2.178′	105° 27.770′	63	10
KRK-12	6° 2.023′	105° 27.450′	27	89
KRK-13	6° 1.990′	105° 27.220′	51	70
KRK-14	6° 3.723′	105° 30.312′	44	55
KRK-15	6° 3.769′	105° 30.840′	45	89
KRK-16	6° 4.800′	105° 31.300′	46	39
KRK-17	6° 4.134′	105° 31.790′	49	81
KRK-18	6° 4.005′	105° 31.450′	51	89
KRK-19	6° 2.930′	105° 30.860′	47	95
KRK-20	6° 2.550′	105° 30.700′	60	67
KRK-21	6° 1.450′	105° 29.100′	52	86
KRK-22	6° 0.680′	105° 25.960′	65	33
KRK-23	6° 0.830′	105° 26.825′	41	78
KRK-24	6° 0.700′	105° 26.600′	34	78
KRK-25	6° 0.700′	105° 26.800′	31	33
KRK-26	6° 5.803′	105° 30.610′	62	85
KRK-27	6° 5.144′	105° 30.323′	66	11
KRK-28	6° 5.130′	105° 24.930′	21	19
KRK-29	6° 5.130′	105° 24.730′	30	13
KRK-30A	6° 4.010′	105° 26.795′	38	55

KRK-30B	6° 4.010′	105° 26.795′	38	12
KRK-31	6° 4.269′	105° ′	35	50
KRK-32A	6° 0.026′	105° 24.771′	61	75.5
KRK-32B	6° 0.026′	105° 24.771′	61	23
KRK-33A	6° 0.000′	105° 25.900′	55	65
KRK-33B	6° 0.000′	105° 25.900′	55	21
KRK-34	6° 0.421′	105° 27.465′	32	24
KRK-35	5° 57.569′	105° 25.906′	69	72
KRK-36	6° 0.000′	105° 28.750′	58	21
KRK-37	6° 3.033′	105° 29.712′	56	38
KRK-38A	6° 2.596′	105° 30.009′	59	60
KRK-38B	6° 2.596′	105° 30.009′	59	10
KRK-39	6° 2.098′	105° 27.562′	30	42
KRK-40	6° 2.237′	105° 26.425′	49	
KRK-41	6° 2.568′	105° 26.643′	60	49
KRK-42	6° 3.917′	105° 24.965′	54	54
KRK-43	6° 4.516′	105° 25.195′	31	70
KRK-44	6°4.055′	105° 29.475′	58	41
KRK-45	6° 3.603′	105° 30.972′	45	30
KRK-46A	6° 4.932′	105° 21.618′	49	63
KRK-46B	6° 4.932′	105° 21.618′	49	17
KRK-47	6° 4.705′	105° 21.553′	56	84
KRK-48	6° 5.350′	105° 21.073′	55	75